

# Baryon Resonances from Electroproduction

Michael Doering

With J. Hergenrather, M. Mai, T. Mart, U.-G. Meißner, D. Roenchen,  
Y.-F. Wang, R. Workman et al.

THE GEORGE  
WASHINGTON  
UNIVERSITY

WASHINGTON, DC

**Jefferson Lab**  
Thomas Jefferson National Accelerator Facility



Department of Energy,  
DOE DE-AC05-06OR23177  
& DE-SC0016582



HPC support by JSC  
grant *jikp07*



National Science Foundation  
Grant No. PHY 2012289



# Degrees of freedom: Quarks or hadrons

---

- Resonance review [[Mai 2022](#)]

# QCD at low energies

Non-perturbative dynamics

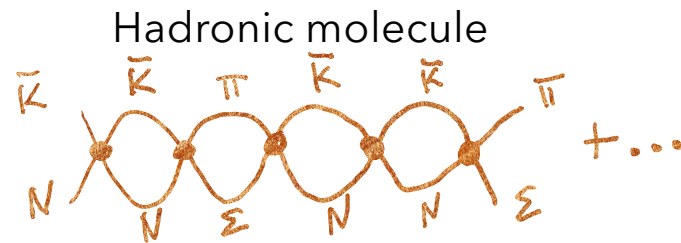
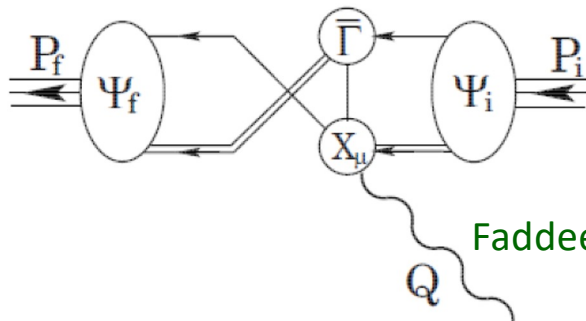
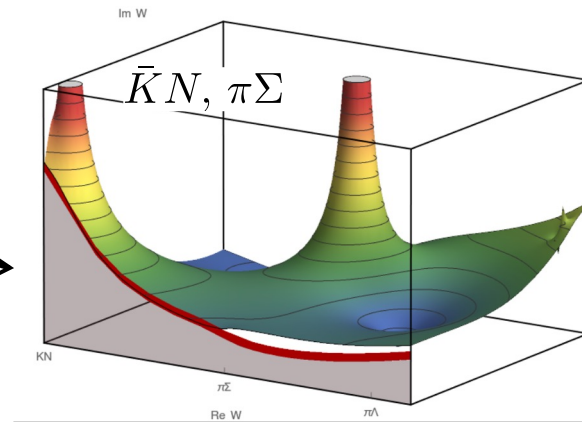
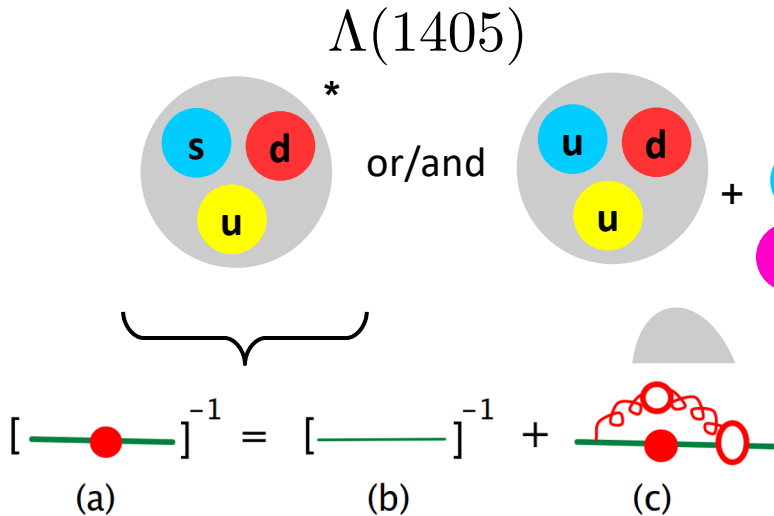
→ rich spectrum of excited states

How many states are there?

→ missing resonance problem (does it exist?)

What are they?

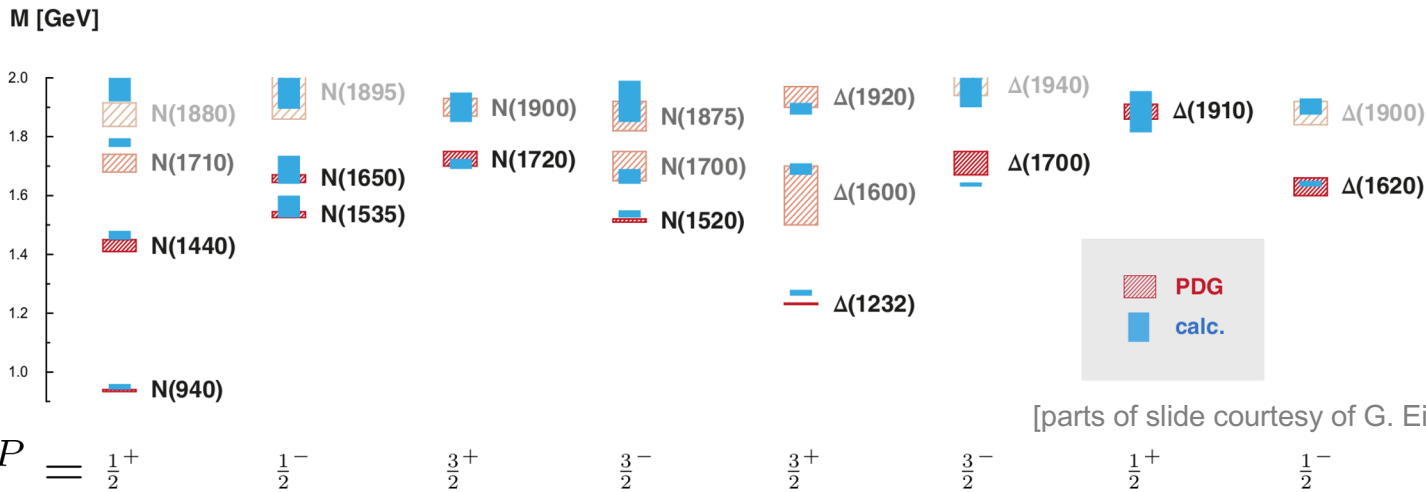
→ 2-quark/3-quark, hadron molecules, ...



Faddeev Eq. / DSE (Binosi, Cloet, Chang, Eichman, Roberts,...);

# Light baryons from diquark dynamics

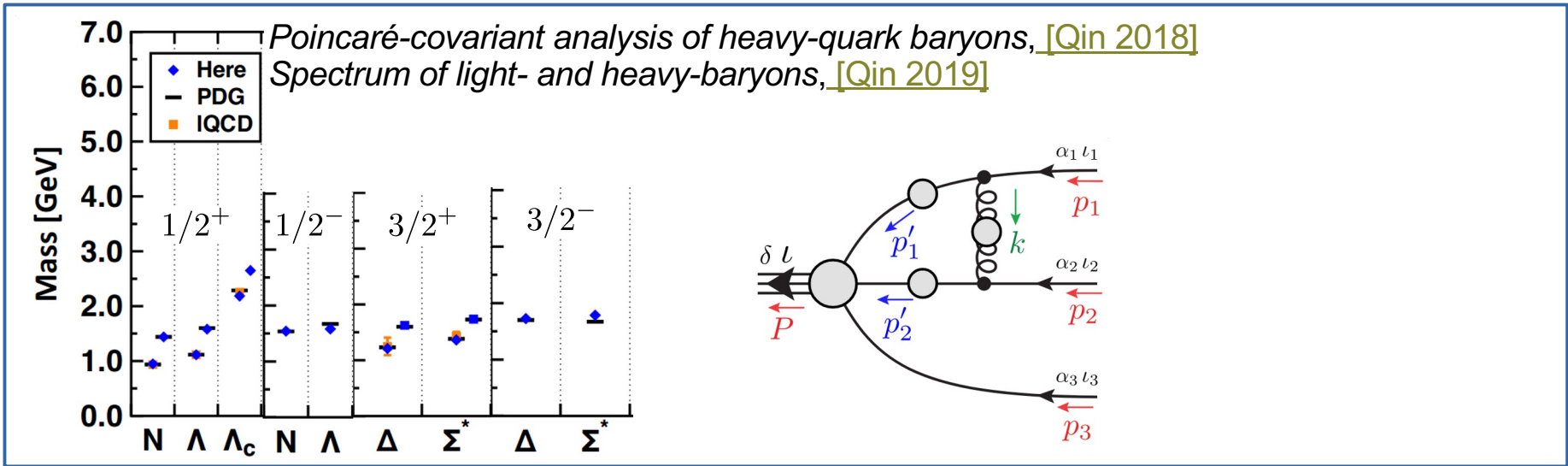
Quark-diquark with reduced pseudoscalar + vector diquarks: [\[Eichmann \(2016\)\]](#)



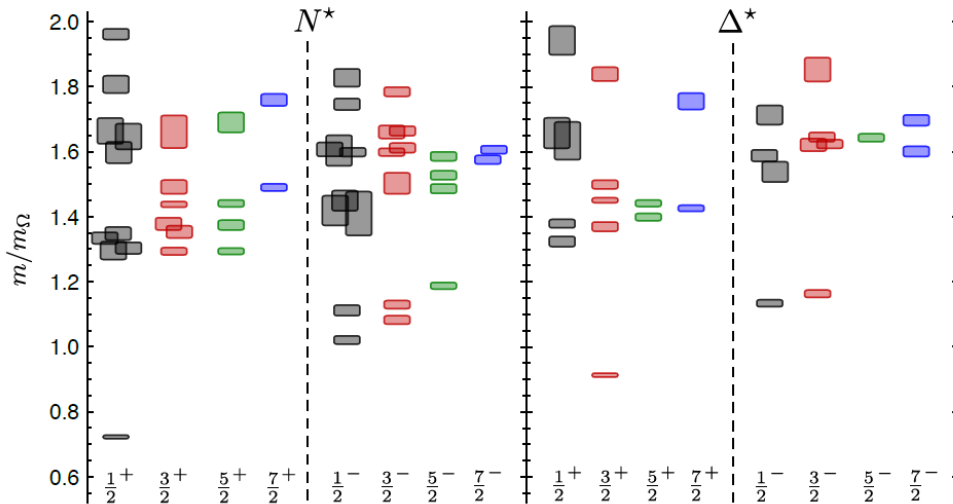
Not much of a missing resonance problem left

[parts of slide courtesy of G. Eichmann, Few Body 2018]

$J^P$

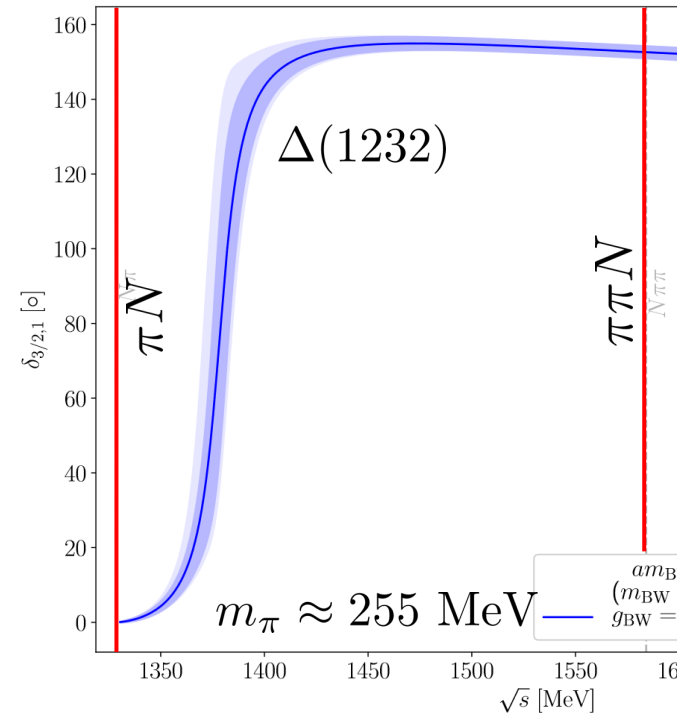


# Lattice QCD for excited baryons



$m_\pi = 396$  MeV [Edwards et al., Phys.Rev. D84 (2011)]

- Information on existence, width & properties of resonances requires
  - Meson-baryon interpolating operators
  - Detailed finite-volume analysis



[G. Silvi et. al., [arXiv: 2101.00689](https://arxiv.org/abs/2101.00689)]

See also: Bulava et al.,  
[[2208.03867](https://arxiv.org/abs/2208.03867)]

How about  $\pi\pi N$ ?  
3B Dynamics?

# Phenomenology of the baryon spectrum

---

Review by [\[Thiel, Afzal, Wunderlich 2022\]](#)

# Dynamical coupled-channel approaches

[MD, M. Mai, J. Haidenbauer, T. Sato, upcoming review]

- ANL-Osaka (former: EBAC) [[Kamano et al.](#)]
- Dubna-Mainz-Taipei model [[Tiator](#)]
- Jülich-Bonn(-Washington) [[Rönchen](#)]
- ...
- Characteristics:
  - Direct fit to data (pion & photon-induced)
  - Simultaneous fit to data of different final states
  - Integral scattering equation as needed for proper treatment of three-body channels ( $\pi\pi N$ ) & inclusion of lefthand cut

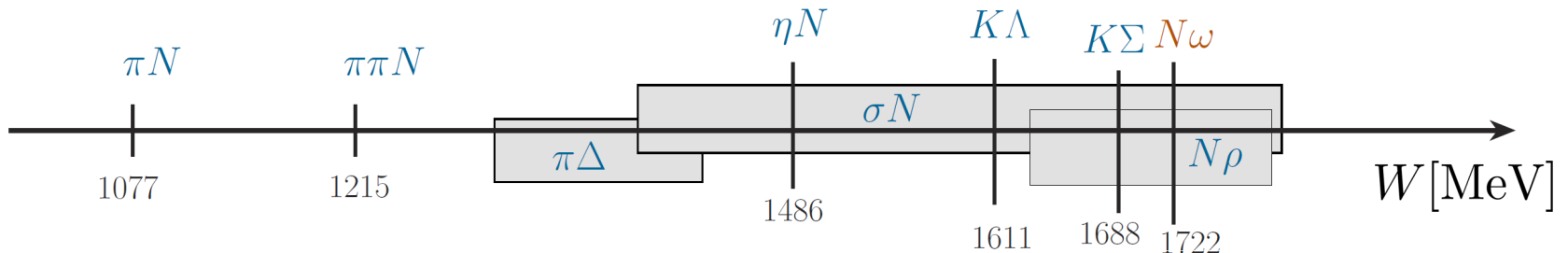
**Note:** Only a subclass of analysis efforts; see, e.g., Bonn-Gatchina group K-matrix approach

# JBW DCC approach (Jülich-Bonn-Washington)

The scattering equation in partial-wave basis

$$\langle L' S' p' | T_{\mu\nu}^{JJ} | L S p \rangle = \langle L' S' p' | V_{\mu\nu}^{JJ} | L S p \rangle + \sum_{\gamma, L'' S''} \int_0^{\infty} dq \, q^2 \langle L' S' p' | V_{\mu\gamma}^{JJ} | L'' S'' q \rangle \frac{1}{E - E_{\gamma}(q) + i\epsilon} \langle L'' S'' q | T_{\gamma\nu}^{JJ} | L S p \rangle$$

■ channels  $\nu, \mu, \gamma$ :

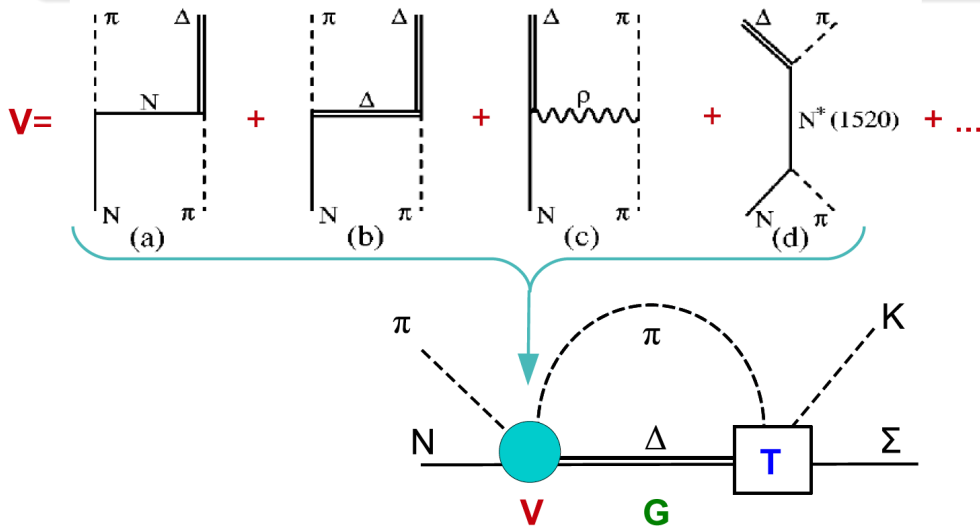




# JBW DCC approach (Jülich-Bonn-Washington)

The scattering equation in partial-wave basis

$$\langle L' S' p' | T_{\mu\nu}^{IJ} | L S p \rangle = \langle L' S' p' | V_{\mu\nu}^{IJ} | L S p \rangle + \sum_{\gamma, L'' S''} \int_0^\infty dq q^2 \langle L' S' p' | V_{\mu\gamma}^{IJ} | L'' S'' q \rangle \frac{1}{E - E_\gamma(q) + i\epsilon} \langle L'' S'' q | T_{\gamma\nu}^{IJ} | L S p \rangle$$



- potentials  $V$  constructed from effective  $\mathcal{L}$
- $s$ -channel diagrams:  $T^P$   
genuine resonance states
- $t$ - and  $u$ -channel:  $T^{NP}$   
dynamical generation of poles  
partial waves strongly correlated
- contact terms

# Transitions in s, t, and u-channels

- 21 s-channel exchanges (resonance)
- Contact terms
- t and u-channel exchanges:

[Yu-Fei Wang 2022]

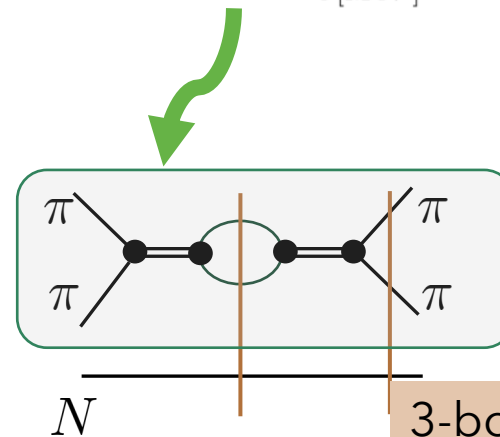
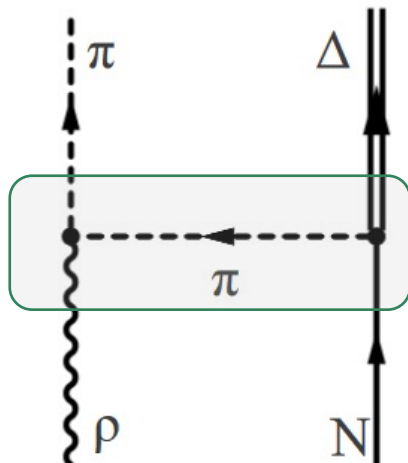
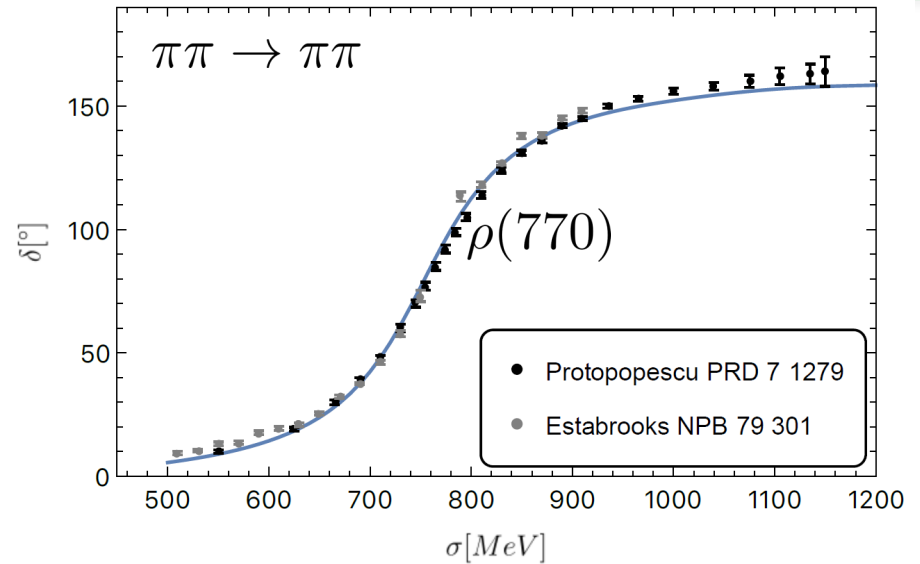
$\mu$	$\pi N$	$\eta N$	$K\Lambda$	$K\Sigma$	$\omega N$	$\pi\Delta$	$\sigma N$	$\rho N$
$\pi N$	$(\pi\pi)_{\sigma},$ $(\pi\pi)_{\rho},$ $N, \Delta$	$a_0, N$	$K^*, \Sigma,$ $\Sigma^*$	$K^*, \Lambda,$ $\Sigma, \Sigma^*$	$\rho, N$	$\rho, N, \Delta$	$\pi, N$	$\pi, \omega,$ $a_1, N,$ $\Delta, C$
$\eta N$		$N, f_0$	$K^*, \Lambda$	$K^*, \Sigma,$ $\Sigma^*$	$\omega, N$			
$K\Lambda$			$\omega, f_0, \phi,$ $\Xi, \Xi^*$	$\rho, a_0,$ $\Xi, \Xi^*$	$K, K^*,$ $\Lambda$			
$K\Sigma$				$\rho, \omega, \phi,$ $f_0, a_0,$ $\Xi, \Xi^*$	$K, K^*,$ $\Sigma, \Sigma^*$			
$\omega N$					$\sigma, N$			
$\pi\Delta$						$\rho, N, \Delta$	$\pi$	$\pi, N$
$\sigma N$							$\sigma, N$	
$\rho N$								$\rho, N,$ $\Delta, C$

$t (N\bar{N} \rightarrow \pi\pi)$        $s (\pi N \rightarrow \pi N)$

# Three-body channels $\sigma N, \pi\Delta, \rho N$

- Resonant sub-channels
- Fit  $2 \rightarrow 2$  amplitude to  $2 \rightarrow 2$  scattering data
- Include as sub-channel in 3-body amplitude:
- **3-body unitarity:** Requires, e.g.

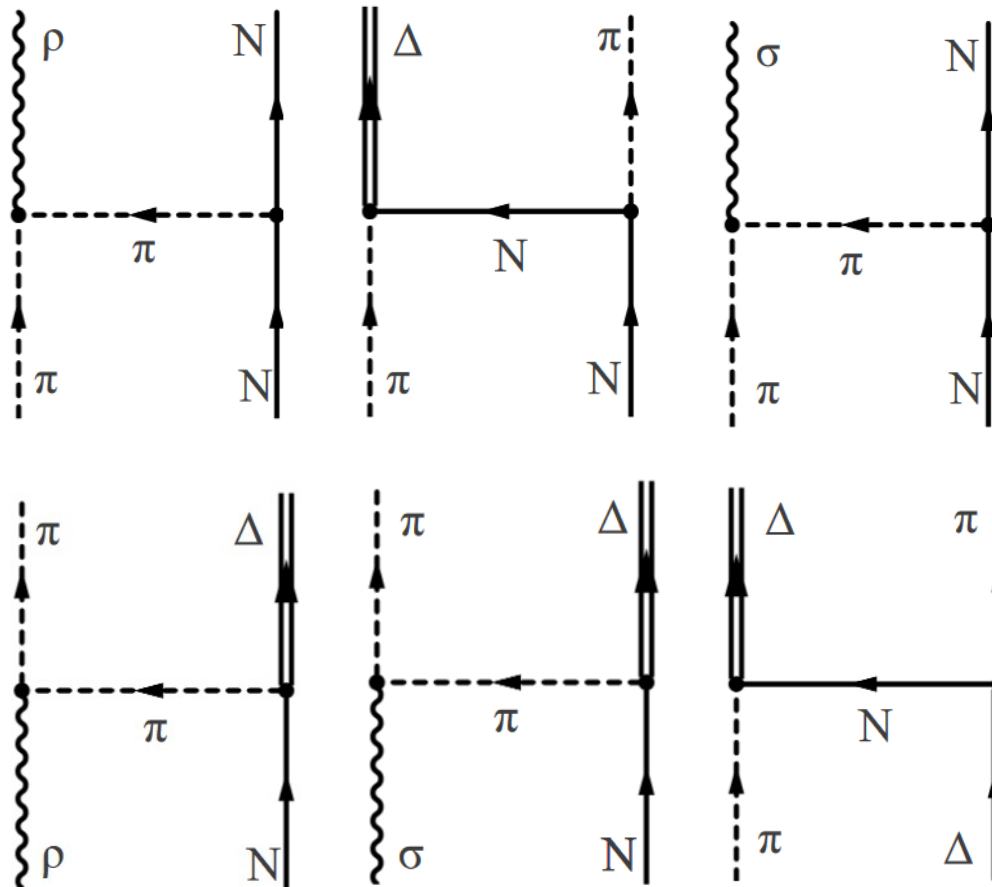


3-body cuts in

- Propagation
- exchange

# 2 → 3 and 3 → 3 body unitarity

- Unitarity requires certain transition amplitudes



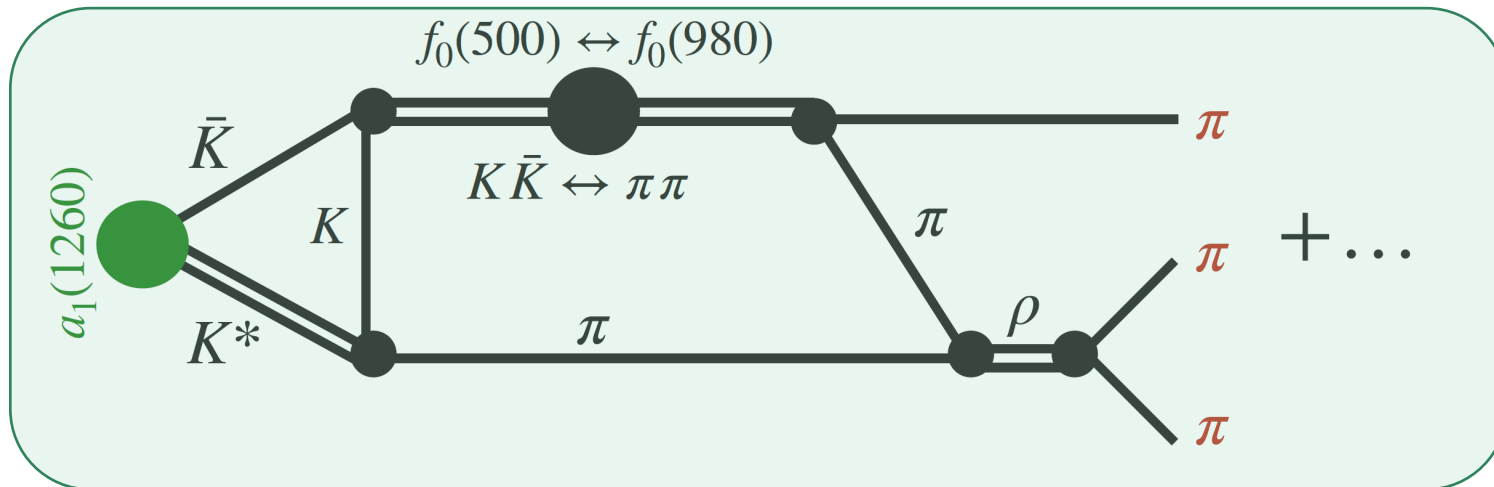
2 → 3

Unitarity requires  
formulation of scattering  
via integral equation  
→ ANL-Osaka & JB(W)


3 → 3

# Unitary amplitudes for meson analysis

[Y. Feng, F. Gil, R. Molina, M. Mai, V. Shastry, A. Szczepaniak, MD]



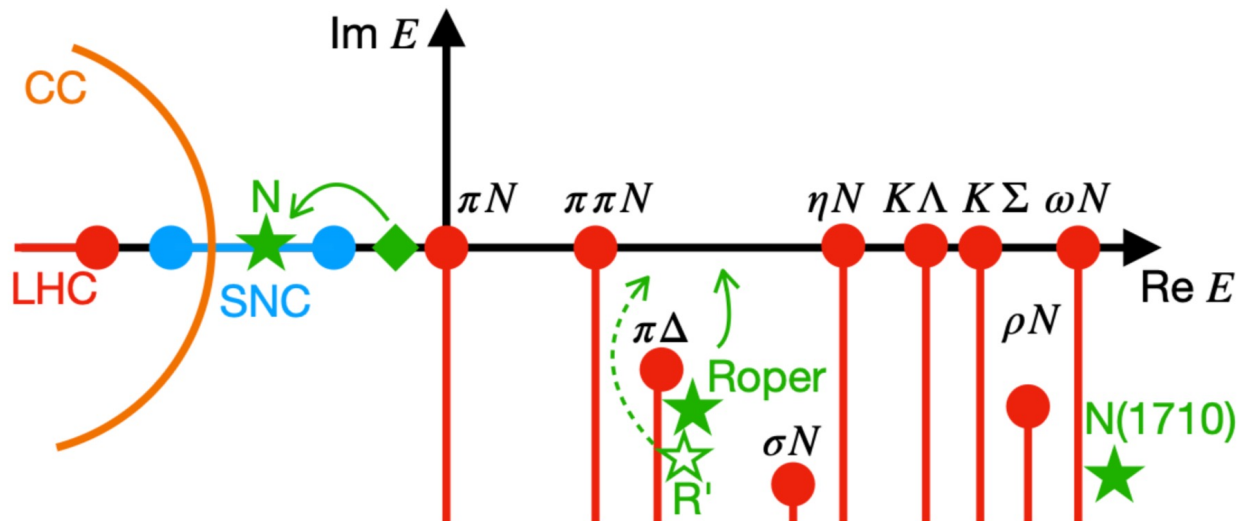
# JB: Data base

- $\pi N \rightarrow X$ : > 7,000 data points ( $\pi N \rightarrow \pi N$ : GW-SAID W108 (ED solution))
- $\gamma N \rightarrow X$ :  **New:  $\pi N \rightarrow \omega N$  [Yu-Fei Wang 2022]**

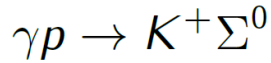
Reaction	Observables (# data points)	p./channel
$\gamma p \rightarrow \pi^0 p$	$d\sigma/d\Omega$ (18721), $\Sigma$ (2927), $P$ (768), $T$ (1404), $\Delta\sigma_{31}$ (140), $G$ (393), $H$ (225), $E$ (467), $F$ (397), $C_{x'_L}$ (74), $C_{z'_L}$ (26)	25,542
$\gamma p \rightarrow \pi^+ n$	$d\sigma/d\Omega$ (5961), $\Sigma$ (1456), $P$ (265), $T$ (718), $\Delta\sigma_{31}$ (231), $G$ (86), $H$ (128), $E$ (903)	9,748
$\gamma p \rightarrow \eta p$	$d\sigma/d\Omega$ (9112), $\Sigma$ (403), $P$ (7), $T$ (144), $F$ (144), $E$ (129)	9,939
$\gamma p \rightarrow K^+ \Lambda$	$d\sigma/d\Omega$ (2478), $P$ (1612), $\Sigma$ (459), $T$ (383), $C_{x'}$ (121), $C_{z'}$ (123), $O_{x'}$ (66), $O_{z'}$ (66), $O_x$ (314), $O_z$ (314),	5,936
$\gamma p \rightarrow K^+ \Sigma^0$	$d\sigma/d\Omega$ (4271), $P$ (422), $\Sigma$ (280), $T$ (127), $C_{x',z'}$ (188), $O_{x,z}$ (254)	5,542
$\gamma p \rightarrow K^0 \Sigma^+$	$d\sigma/d\Omega$ (242), $P$ (78)	320
	in total	<b>57,027</b>

# Partial-Wave Analytic structure

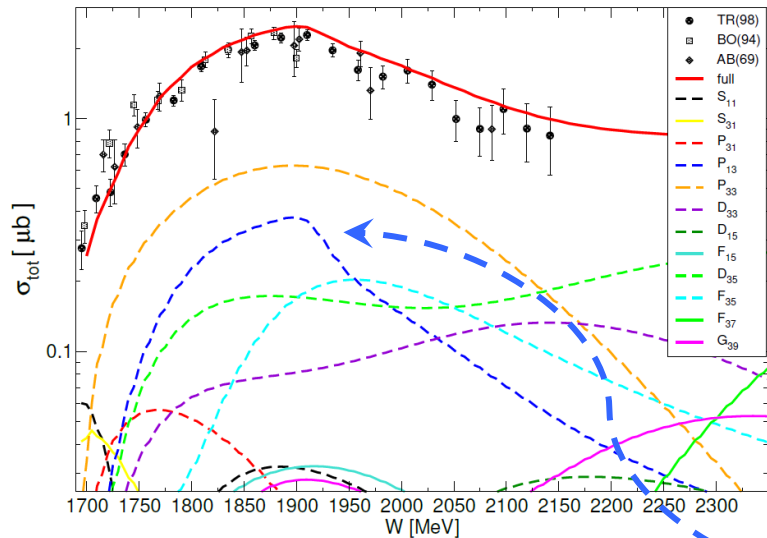
- Branch points indicate thresholds
- Partial-wave amplitudes have more cuts than plane-wave amplitude
- Example: The structure of the P11 amplitude



# Resonances in $K\Sigma$ photoproduction



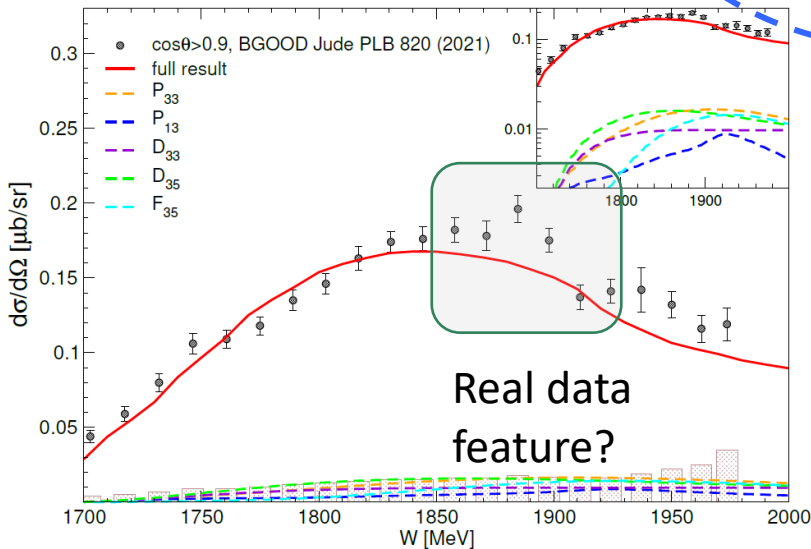
- [\[D. Roenchen et al. \(EPJA 2022\)\]](#)
- [\[Webpage all results\]](#)



dominant partial waves:  $l = 3/2$

Exception:  $P_{13}$  partial wave ( $l = 1/2$ ):

$N(1720) 3/2^+$ * * *	Re $E_0$ [MeV]	$-2\text{Im } E_0$ [MeV]	$\frac{\Gamma_{\pi N}^{1/2} \Gamma_{K\Sigma}^{1/2}}{\Gamma_{\text{tot}}}$ [%]	$\theta_{\pi N \rightarrow K\Sigma}$ [deg]
2022	1726	185	5.9	82
2017	1689(4)	191(3)	0.6(0.4)	26(58)
PDG 2021	$1675 \pm 15$	$250^{+150}_{-100}$	—	—



Real data  
feature?

Similarly:  $K^0 \Sigma^+$

$N(1900) 3/2^+$ * * *	Re $E_0$ [MeV]	$-2\text{Im } E_0$ [MeV]	$\frac{\Gamma_{\pi N}^{1/2} \Gamma_{K\Sigma}^{1/2}}{\Gamma_{\text{tot}}}$ [%]	$\theta_{\pi N \rightarrow K\Sigma}$ [deg]
2022	1905	93	1.3	-40
2017	1923(2)	217(23)	10(7)	-34(74)
PDG 2021	$1920 \pm 20$	$150 \pm 50$	$4 \pm 2$	$110 \pm 30$

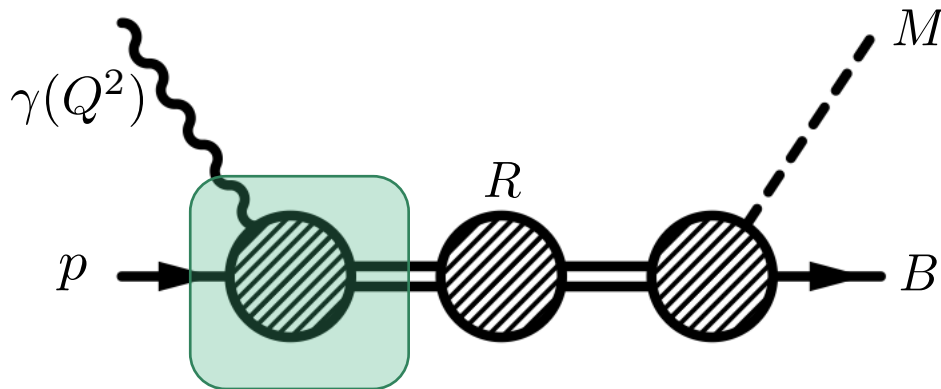
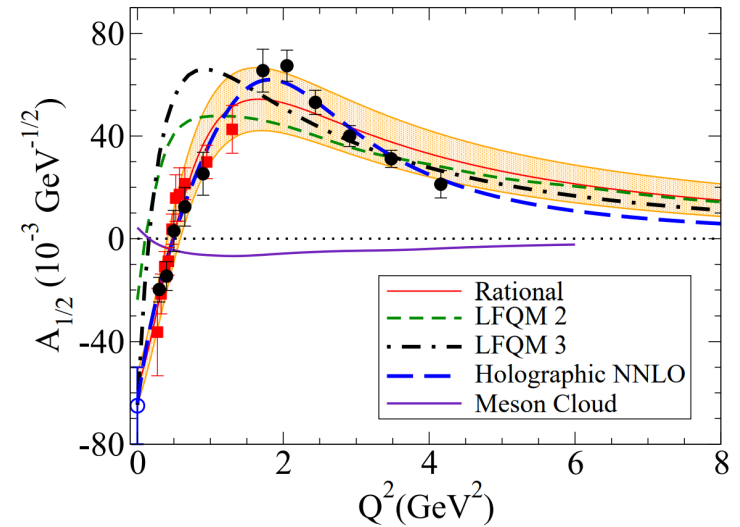
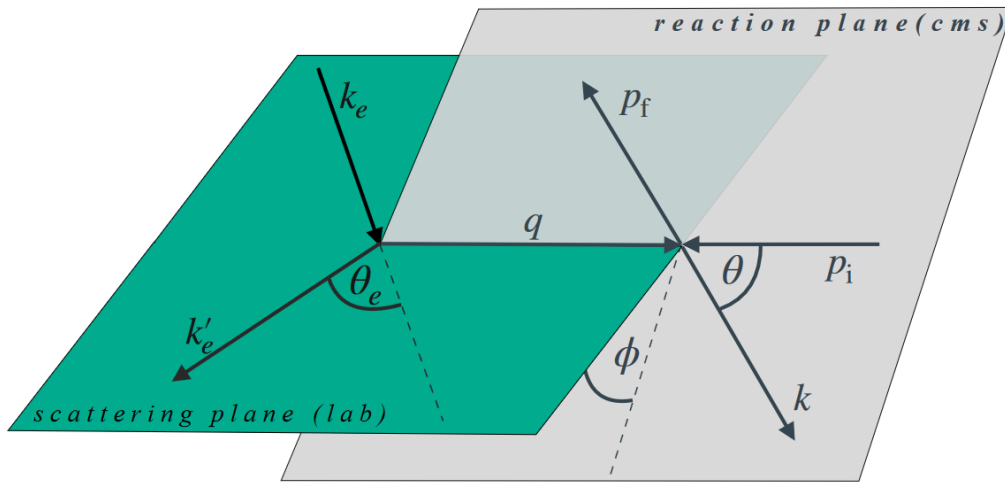
drop in cross section (“cusp-like structure”) due to  $N(1900)3/2^+$

$N(1535) 1/2^-$ * * *	Re $E_0$ [MeV]	$-2\text{Im } E_0$ [MeV]
2022	1504(0)	74 (1)
2017	1495(2)	112(1)
PDG 2021	$1510 \pm 10$	$130 \pm 20$

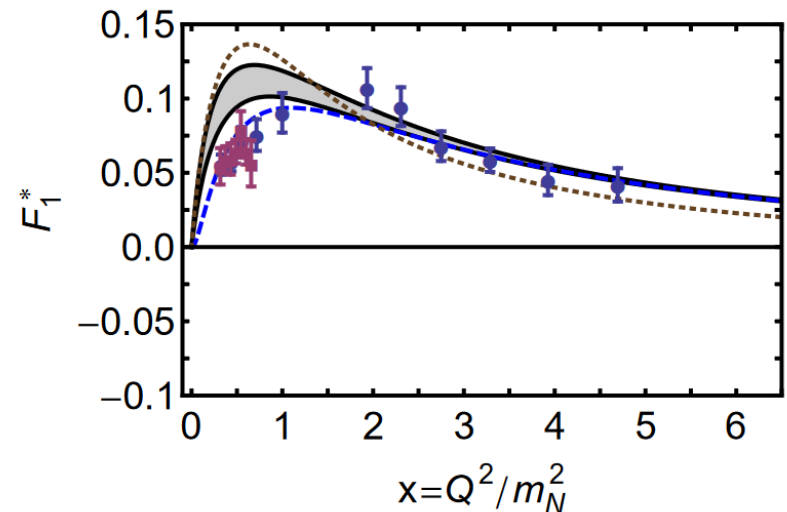
New, wide  
dynamically  
generated  
states in  $J^P=3/2^-$



# Electroproduction reveals resonance structure



Reaction-independent transition form factor at resonance pole

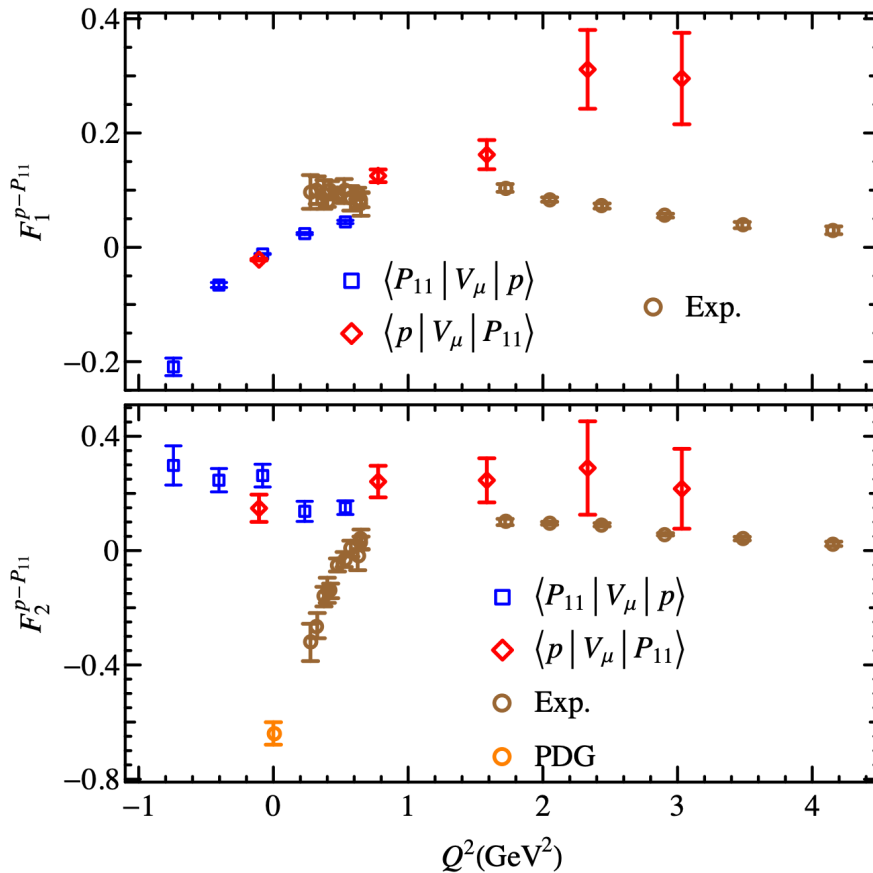


Proton-Roper Transition [[Burkert](#)] [[Segovia](#)]

# Baryon TFFs from Lattice

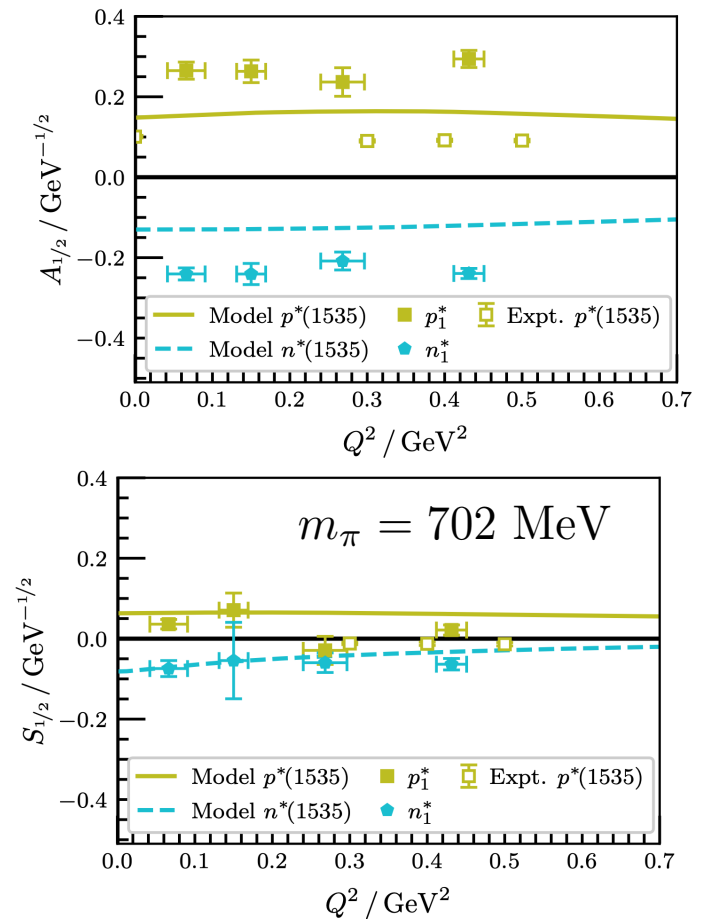
- Proton-Roper

[H.-W. Lin et al. (2008)]



- N(1535)1/2-

[F.-M. Stokes et al. (2024)]



# Electroproduction Analysis Efforts

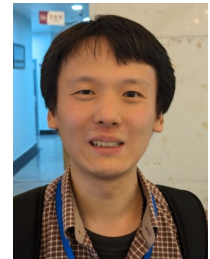
- **MAID**: electroproduction of pions, eta mesons, and kaons in separate approaches [[Tiator 2007](#)]
- **JM (JLab)** approach: single-pion analysis, double pion analysis [[Moiseev, PRC 2023](#)]; Jlab unitary isobar (**UI**) analysis
- **ANL-Osaka**: Single-pion electroproduction, using multi-channel model. [[Kamano, Lee, Nakamura, Sato, 2016](#)]
- **JBW**: simultaneous analysis of multiple electroproduction final states, using multi-channel model
- **Bonn-Gatchina** (upcoming)



J. Hergenrather



M. Mai



Yu-Fei Wang

# Coupled-Channel Electroproduction

First coupled-channel electroproduction analysis of different final states

---

(2020-)

# Formalism

- Photoproduction solution as constraint
- Constraints from (Pseudo)-threshold:

$(E_{l+}^I, L_{l+}^I) \rightarrow k^l q^l \quad (l \geq 0)$ $(M_{l+}^I, M_{l-}^I) \rightarrow k^l q^l \quad (l \geq 1)$ $(L_l^I) \rightarrow kq \quad (l = 1)$ $(E_{l-}^I, L_{l-}^I) \rightarrow k^{l-2} q^l \quad (l \geq 2)$	$k =  \mathbf{k}  = \frac{\sqrt{((W - M_N)^2 + Q^2) ((W + M_N)^2 + Q^2)}}{2W}$ $q =  \mathbf{q}  = \frac{\sqrt{((W - M_N)^2 - M_m^2) ((W + M_N)^2 - M_m^2)}}{2W}$
--	---

- Siegert's theorem

$\frac{E_{l+}}{L_{l+}} \rightarrow 1,$	$\frac{E_{l-}}{L_{l-}} \rightarrow \frac{-l}{l-1}$
--	--

Amaldi, Fubini, Furlan,  
 Springer Tracts Mod. Phys. 83, 1 (1979)  
 Tiator, Few-body Systems 57, 1087 (2016)

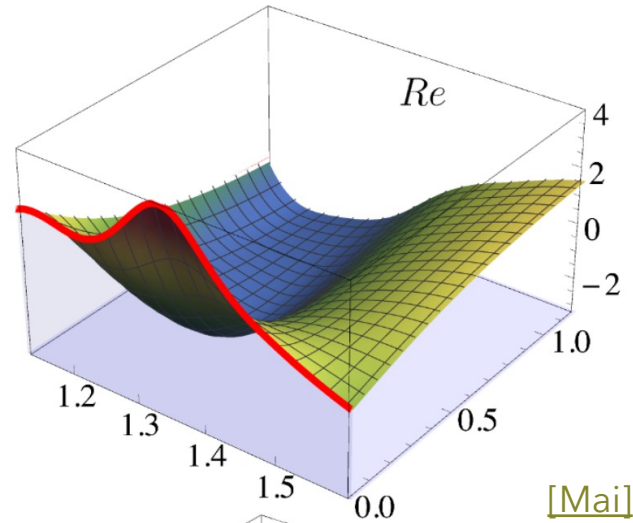
at pseudo-threshold

- Watson's theorem, multi-channel unitarity

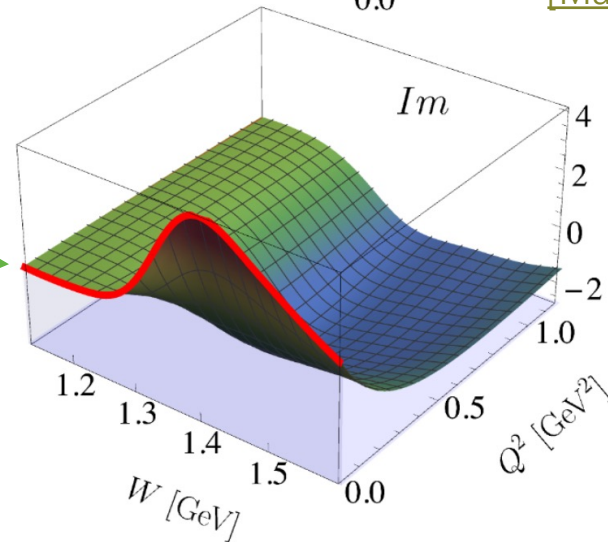
$M_{\mu\gamma^*}(q, W, Q^2) = V_{\mu\gamma^*}(q, W, Q^2) + \sum_{\kappa} \int dp p^2 T_{\mu\kappa}(q, p, W) G_{\kappa}(p, W) V_{\nu\gamma^*}(p, W, Q^2)$	Resonances, background, channels have independent $Q^2$ dependence for flexible fit
$V_{\mu\gamma^*}(p, W, Q^2) = \alpha_{\mu\gamma^*}^{NP}(p, W, Q^2) + \sum_i \frac{\gamma_{\mu;i}^a(p) \gamma_{\gamma^*;i}^c(W, Q^2)}{W - m_i^b}$	

# Photoproduction boundary

$$M_{1-}^{1/2} (N(1440))$$



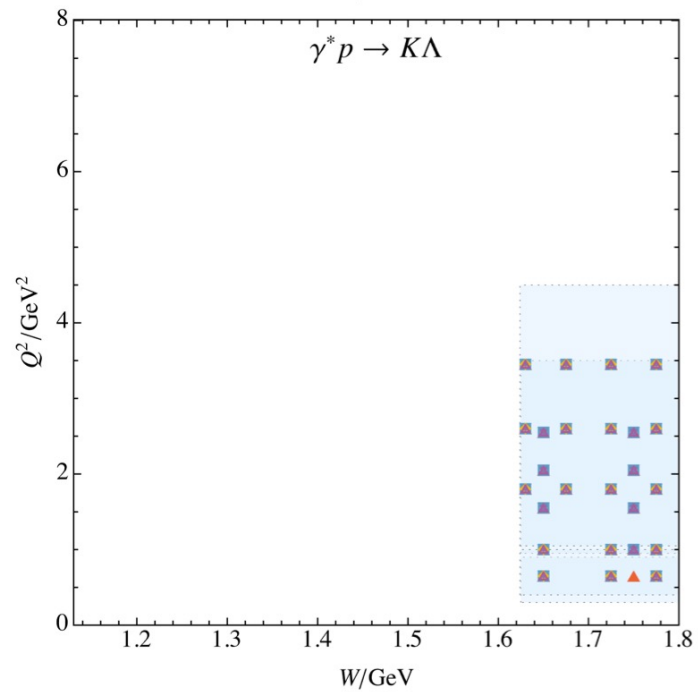
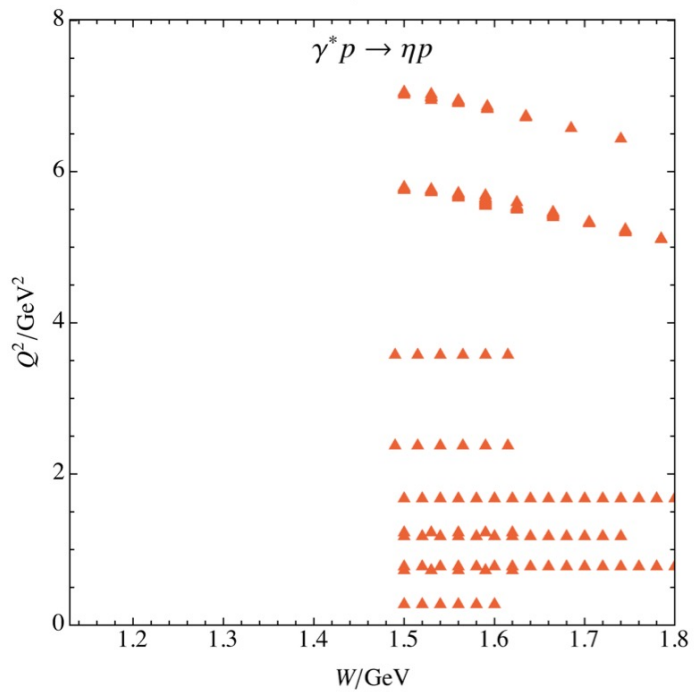
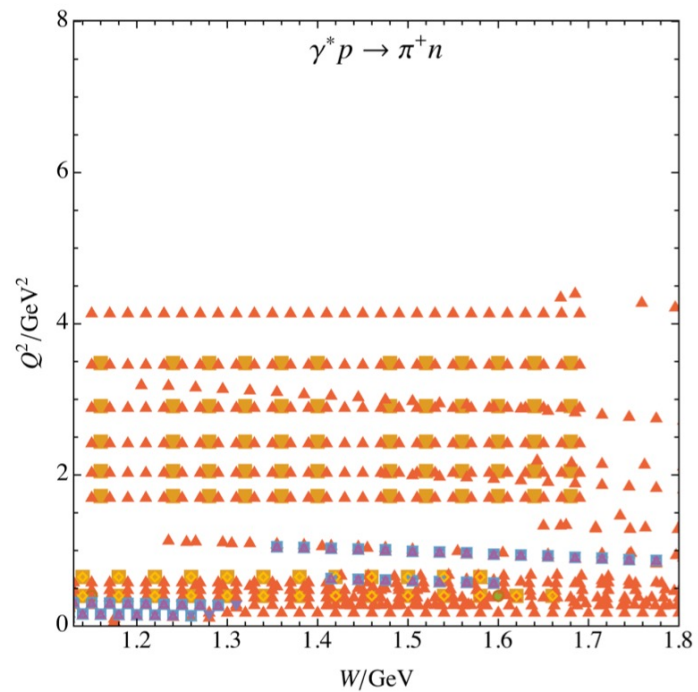
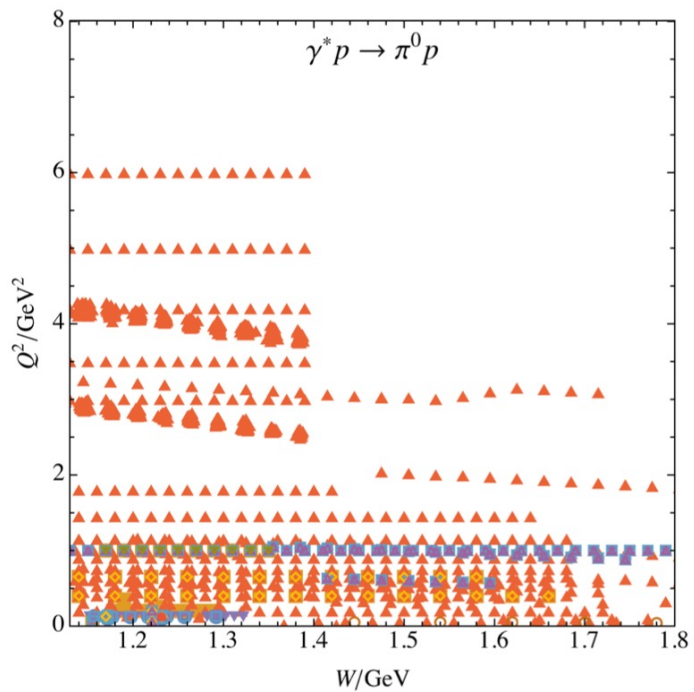
Photoproduction included as boundary



# JBW Electroproduction data base

Type	$N_{\text{data}}^{\pi^0 p}$	$N_{\text{data}}^{\pi^+ n}$	$N_{\text{data}}^{\eta p}$	$N_{\text{data}}^{K\Lambda}$
● $\rho_{LT}$	45	—	—	—
■ $\rho_{LT'}$	2768	5068	—	—
◆ $\sigma_L$	—	2	—	—
▲ $d\sigma/d\Omega$	48135	44266	3665	2055
▼ $\sigma_T + \epsilon\sigma_L$	384	182	—	204
○ $\sigma_T$	30	2	—	—
□ $\sigma_{LT}$	373	138	—	204
◇ $\sigma_{LT'}$	214	208	—	156
△ $\sigma_{TT}$	327	123	—	204
▽ $K_{D1}$	1527	—	—	—
● $P_Y$	—	2	—	—
Total	53804	49989	3665	2823

- Data base grown over decades with recent input mostly by CLAS, MAMI.
- Far from complete: Kinematic gaps & consistency issues. Need to combine information from different ( $W, Q^2$ ) regions
- Need to combine information from simultaneous analysis of different final states ( $\pi N/\eta N/K Y/\pi\pi N, \dots$ ) to extract resonance helicity couplings





# Fit details: Weighted vs. unweighted $\chi^2$

- Meson production data bases are heterogeneous:
  - A few polarization measurements with large error bars (small weight in  $\chi^2$ )
  - Many cross section data with smaller error bars (large weight in  $\chi^2$ )
  - ... but those **few** polarization possess **great** power to discriminate solutions
- Introduce **weighted** vs. **unweighted**  $\chi^2$ :

$$\chi_{\text{wt}}^2 = \sum_{j \in \{\pi^0 p, \pi^+ n, \eta p\}} \frac{N_{\text{all}}}{3N_j} \sum_{i=1}^{N_j} \left( \frac{\mathcal{O}_{ji}^{\text{exp}} - \mathcal{O}_{ji}}{\Delta_{ji}^{\text{stat}} + \Delta_{ji}^{\text{syst}}} \right)^2.$$

$$\chi_{\text{reg}}^2 = \sum_{i=1}^{N_{\text{all}}} \left( \frac{\mathcal{O}_i^{\text{exp}} - \mathcal{O}_i}{\Delta_i^{\text{stat}} + \Delta_i^{\text{syst}}} \right)^2$$

- Quote results for both cases

# Fit Strategies ( $\pi N$ )

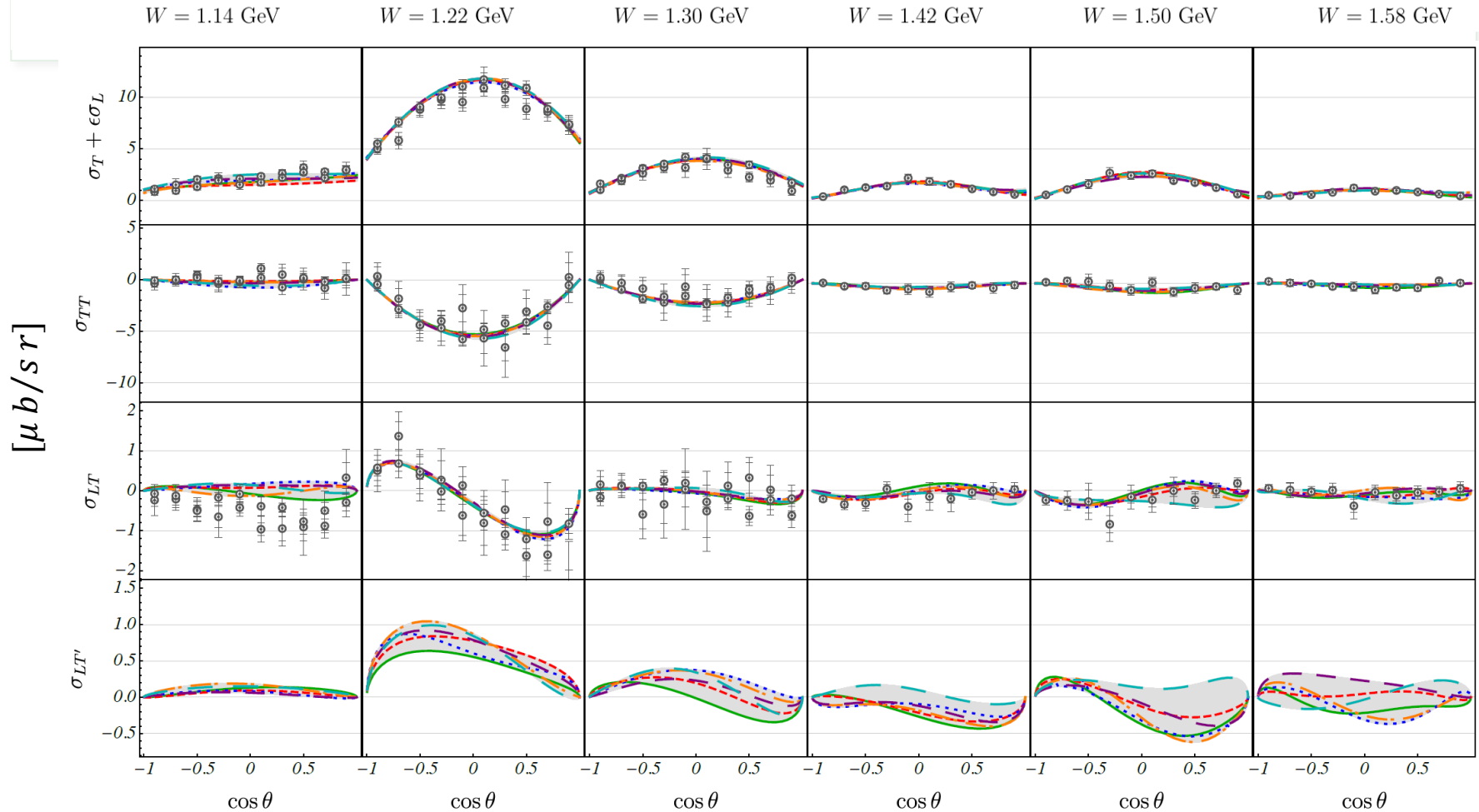
[M. Mai et al, 2021]

- Different fit strategies for  $N \approx 85,000$  data in  $\gamma^* N \rightarrow \pi N, \eta N$ :
  - Sequential  $S \rightarrow S+P \rightarrow S+P+D$  waves;
  - Subsets of data until full data set reached
  - Simultaneous fit all parameters (209) set to zero without any (!) guidance
  - Extend data range from  $0 < Q^2 < 4 \text{ GeV}^2$  to  $0 < Q^2 < 6 \text{ GeV}^2$  to check for stability

Fit	$\sigma_L$		$d\sigma/d\Omega$		$\sigma_T + \epsilon\sigma_L$		$\sigma_T$		$\sigma_{LT}$		$\sigma_{LT'}$		$\sigma_{TT}$		$K_{D1}$		$P_Y$		$\rho_{LT}$		$\rho_{LT'}$		$\chi^2_{\text{dof}}$
	$\pi^0 p$	$\pi^+ n$	$\pi^0 p$	$\pi^+ n$	$\pi^0 p$	$\pi^+ n$	$\pi^0 p$	$\pi^+ n$	$\pi^0 p$	$\pi^+ n$	$\pi^0 p$	$\pi^+ n$	$\pi^0 p$	$\pi^+ n$	$\pi^0 p$	$\pi^+ n$	$\pi^0 p$	$\pi^+ n$	$\pi^0 p$	$\pi^+ n$	$\pi^0 p$	$\pi^+ n$	
$\mathfrak{F}_1$	–	9	65355	53229	870	418	87	88	1212	133	862	762	4400	251	4493	–	234	–	525	–	3300	10294	1.77
$\mathfrak{F}_2$	–	4	69472	55889	1081	619	65	78	1780	150	1225	822	4274	237	4518	–	325	–	590	–	3545	10629	1.69
$\mathfrak{F}_3$	–	8	66981	54979	568	388	84	95	1863	181	1201	437	3934	339	4296	–	686	–	687	–	3556	9377	1.81
$\mathfrak{F}_4$	–	22	63113	52616	562	378	153	107	1270	146	1198	1015	4385	218	5929	–	699	–	604	–	3548	11028	1.78
$\mathfrak{F}_5$	–	20	65724	53340	536	528	125	81	1507	219	1075	756	4134	230	5236	–	692	–	554	–	3580	11254	1.81
$\mathfrak{F}_6$	–	18	71982	58434	1075	501	29	68	1353	135	1600	1810	3935	291	5364	–	421	–	587	–	3932	11475	1.78

$\chi^2$

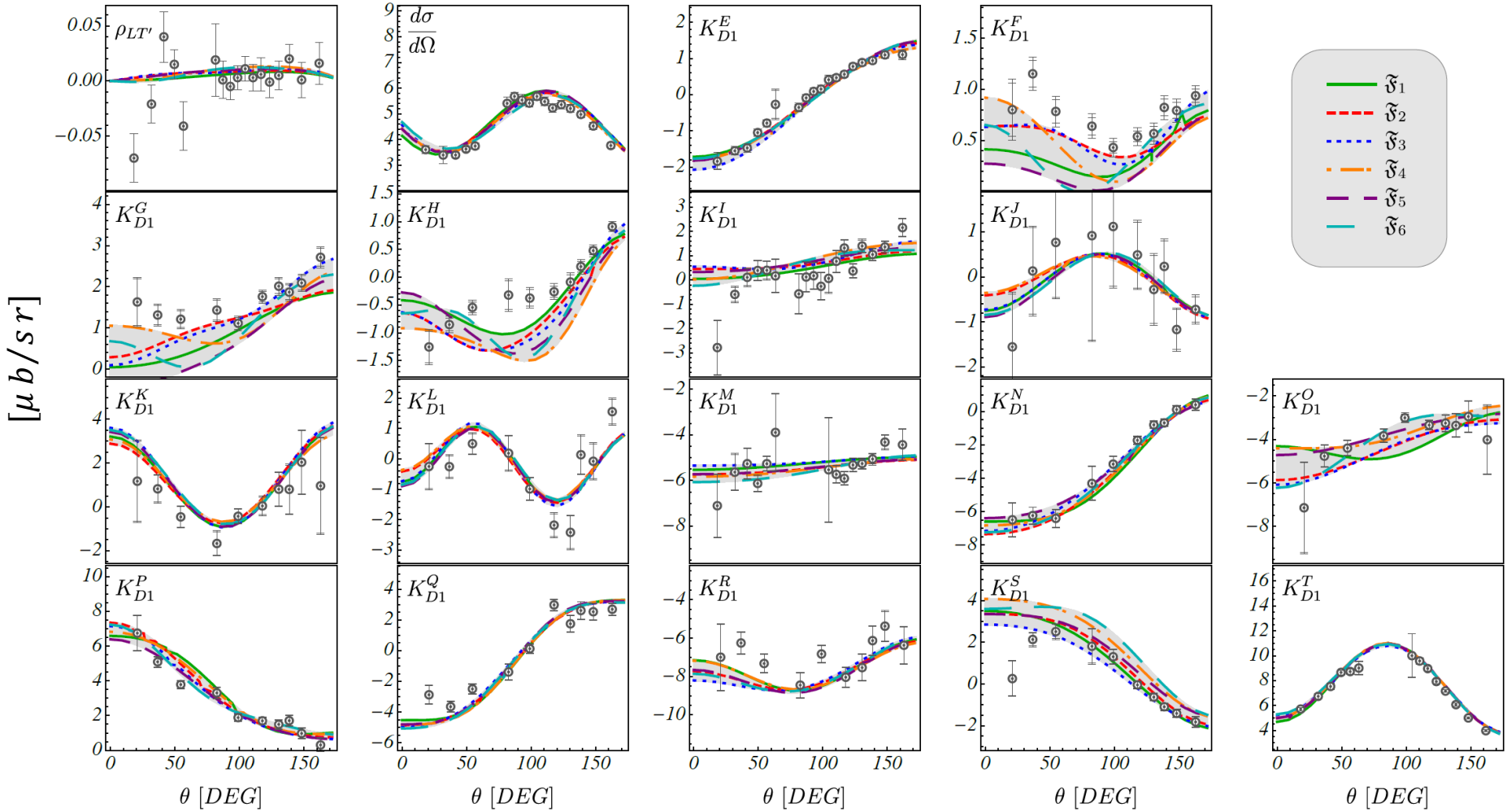
# Structure functions $\pi^0 p$ (not fitted)



$$Q^2 = 0.9 \text{ GeV}^2$$

Data: CLAS, Phys. Rev. C (2003) [0301012 \[nucl-ex\]](#), Phys. Rev. Lett. (2002) [0110007 \[hep-ex\]](#)

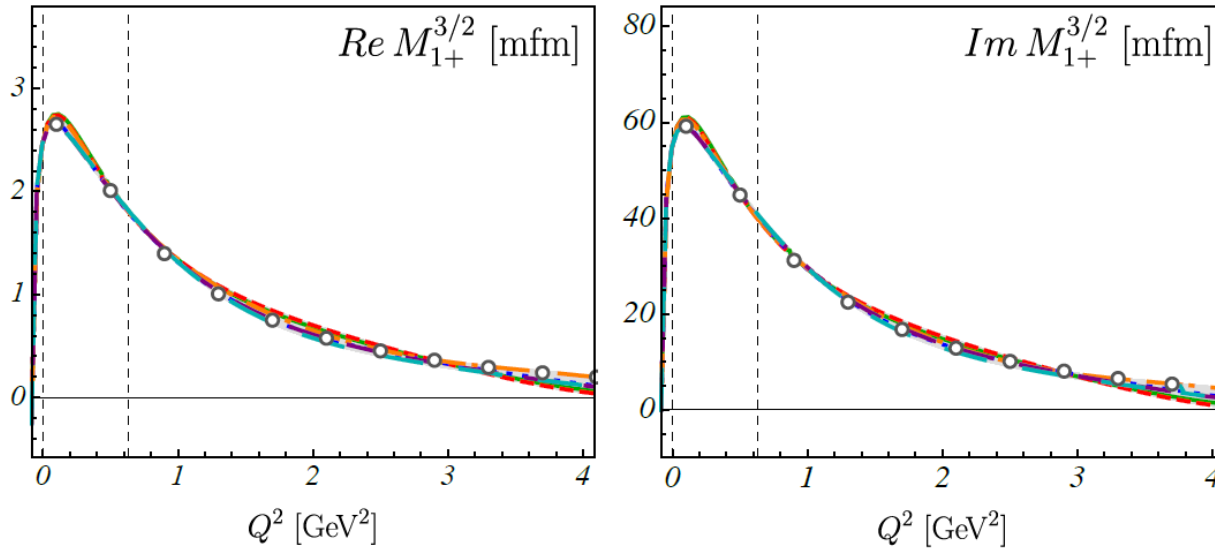
# Description of Polarization Observables ( $\pi N$ )



$\pi^0 p, Q^2=1 \text{ GeV}^2, W=1.23 \text{ GeV}, \phi=15^\circ$

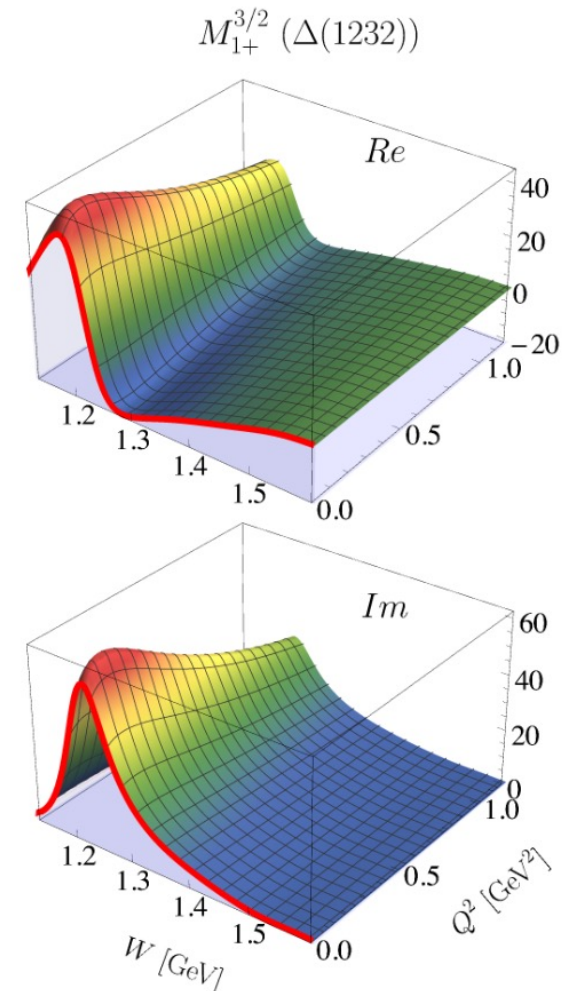
J. J. Kelly, [Phys. Rev. Lett. 95 \(2005\)](#).

# Large Multipoles



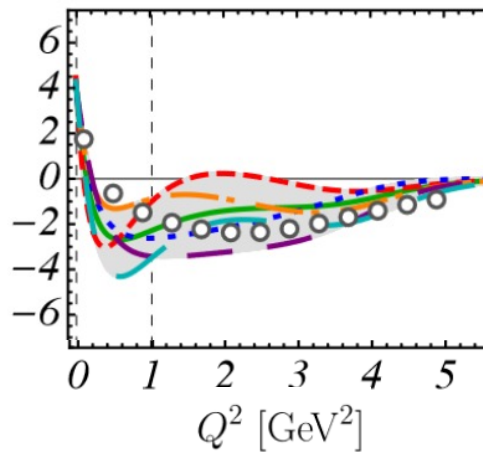
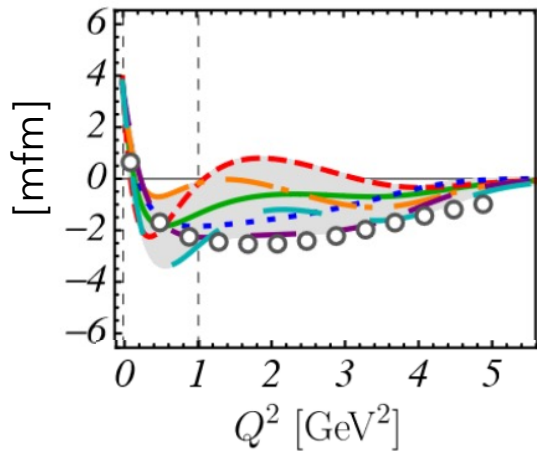
Fit strategies 1-6 together with MAID (open dots) for the magnetic multipole of the  $\Delta(1232)$  Drechsel et al., EPJA (2007) [0710.0306](#) [nucl-th]

**Prominent multipoles are well determined**



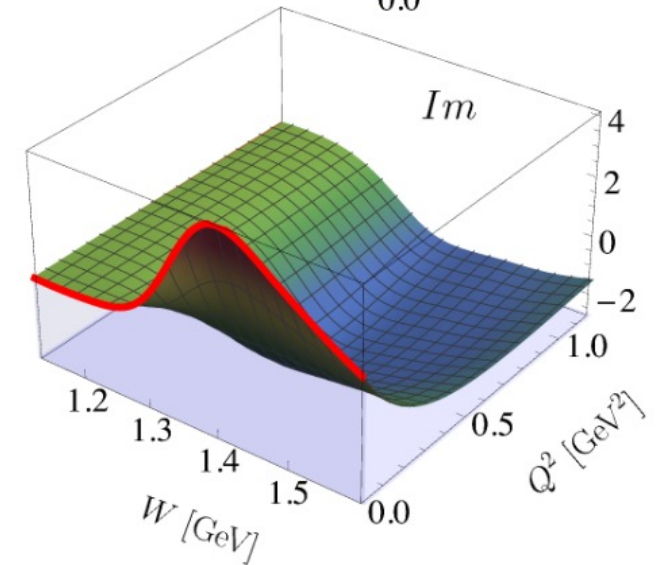
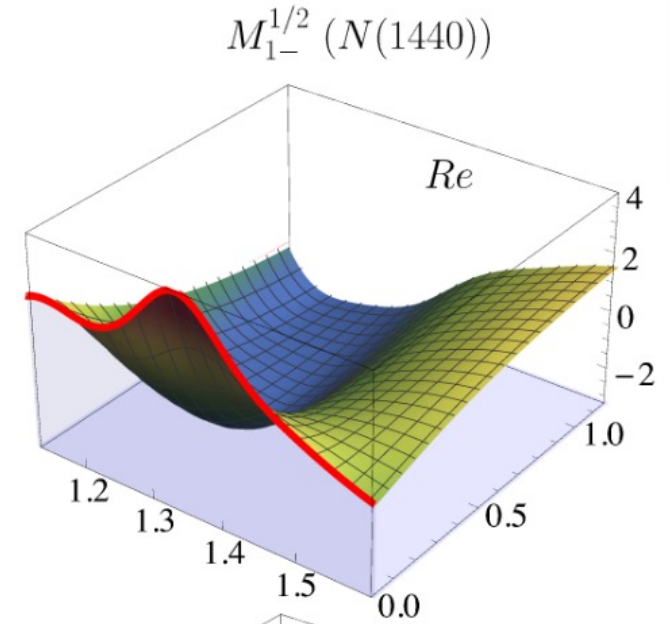
(Strategy 1 only)

# Roper Multipole



( $W=1.38$  GeV fixed)

- Zero-transition (agrees with MAID)
- Extensive exploration of parameter space reveals ambiguities in PWA and reflects systematic uncertainties



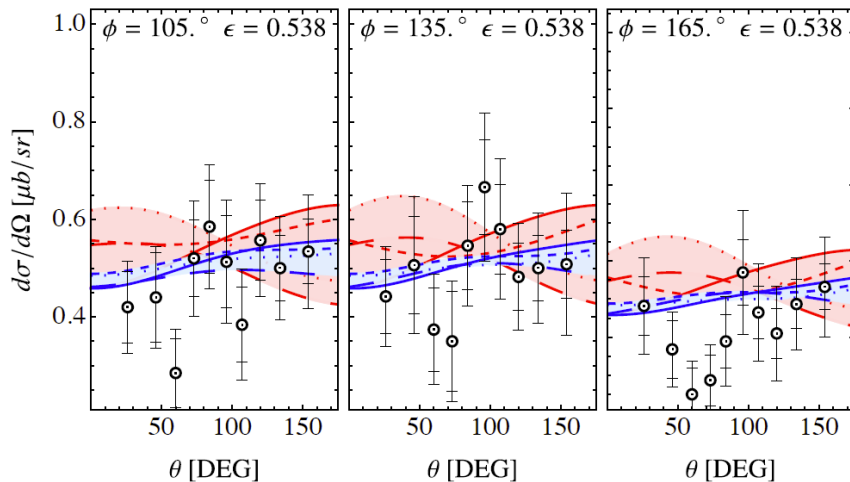
(Strategy 1 only)

# $\eta$ Electroproduction

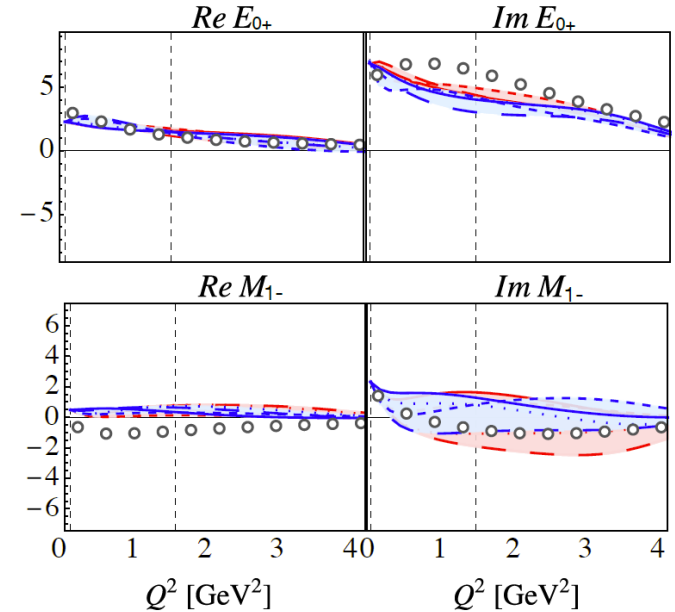
[M. Mai et al., [PRC \(2022\)](#)]

- $N_{data}^{\eta p} = 1,874$  (only  $d\sigma/d\Omega$ ) (84,842 in total)
- kinematic range:  $0 < Q^2 < 4 \text{ GeV}^2$ ,  $1.13 < W < 1.6 \text{ GeV}$
- 8 different fit strategies: 4 with standard  $\chi^2$ , 4 with weighted  $\chi^2$  to account for the smaller  $N_{data}^{\eta p}$   
 → better data description with weighted fit strategies:

Selected fit results:  $\gamma^* p \rightarrow \eta p$  at  $W = 1.5 \text{ GeV}$ ,  
 $Q^2 = 1.2 \text{ GeV}^2$ . Data: Denizli et al. (CLAS) PRC 76 (2007)



Selected multipoles at  $W = 1535 \text{ MeV}$



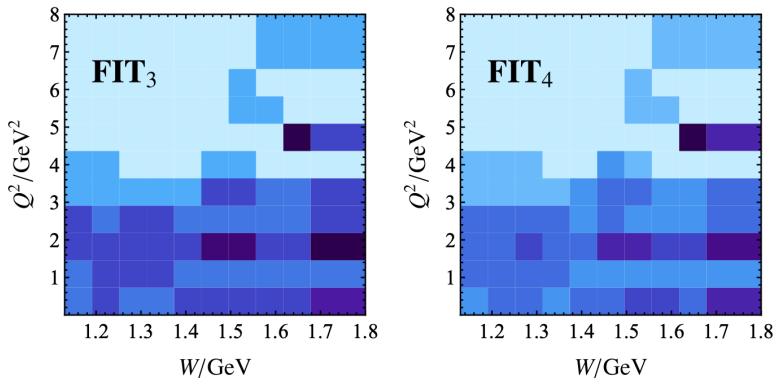
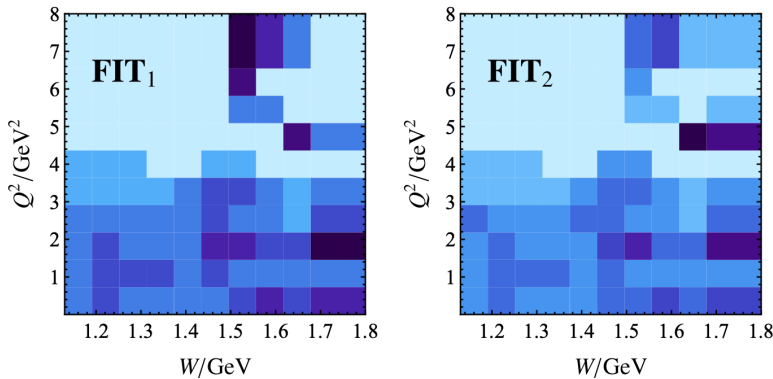
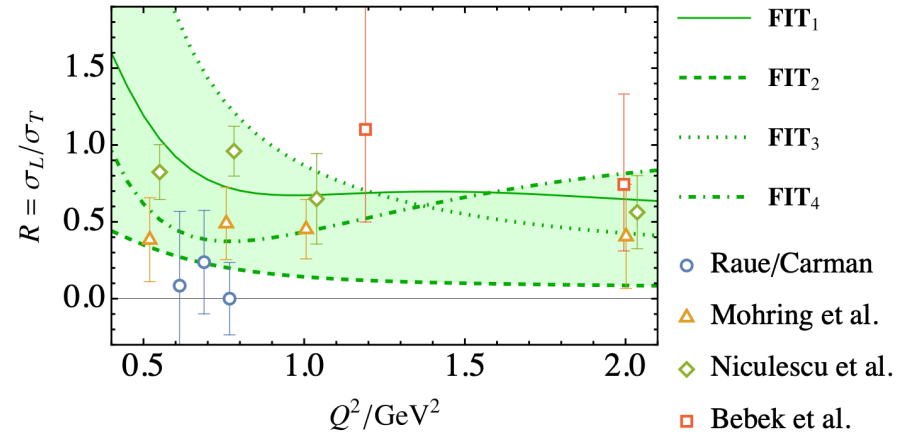
**Upcoming:** Polarization observables! Izzy Illari/CLAS

Dots: eta-MAID, [arXiv:0110034](#)

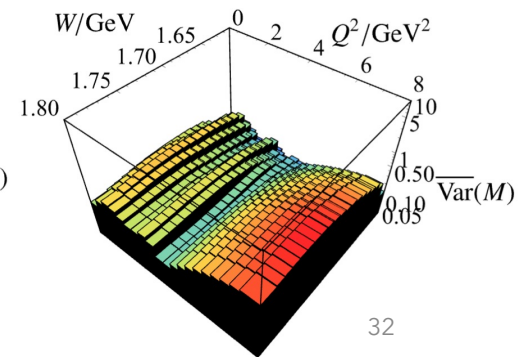
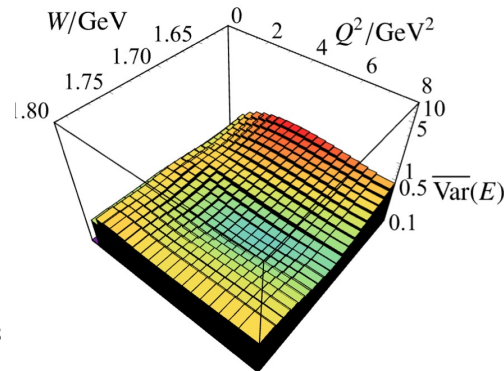
# Kaon electroproduction

[M. Mai et al., EPJA 2023]

	$\chi_{\text{dof}}^2$	$\chi_{\text{pp}}^2(\pi^0 p)$	$\chi_{\text{pp}}^2(\pi^+ n)$	$\chi_{\text{pp}}^2(\eta p)$	$\chi_{\text{pp}}^2(K^+ \Lambda)$
<b>FIT<sub>1</sub></b>	1.42	1.40	1.47	1.49	0.70
<b>FIT<sub>2</sub></b>	1.35	1.38	1.35	1.40	0.58
	$\chi_{\text{wt,dof}}^2$	$\chi_{\text{pp}}^2(\pi^0 p)$	$\chi_{\text{pp}}^2(\pi^+ n)$	$\chi_{\text{pp}}^2(\eta p)$	$\chi_{\text{pp}}^2(K^+ \Lambda)$
<b>FIT<sub>3</sub></b>	1.12	1.44	1.61	1.08	0.33
<b>FIT<sub>4</sub></b>	1.06	1.42	1.44	1.09	0.32



$$\overline{\text{Var}}(W, Q^2)(X) := \sum_{\ell_{\pm}} \frac{\text{Var}\{|X_{\ell_{\pm}, i}|\}}{\text{Mean}\{|X_{\ell_{\pm}, i}|\} + \varepsilon}$$

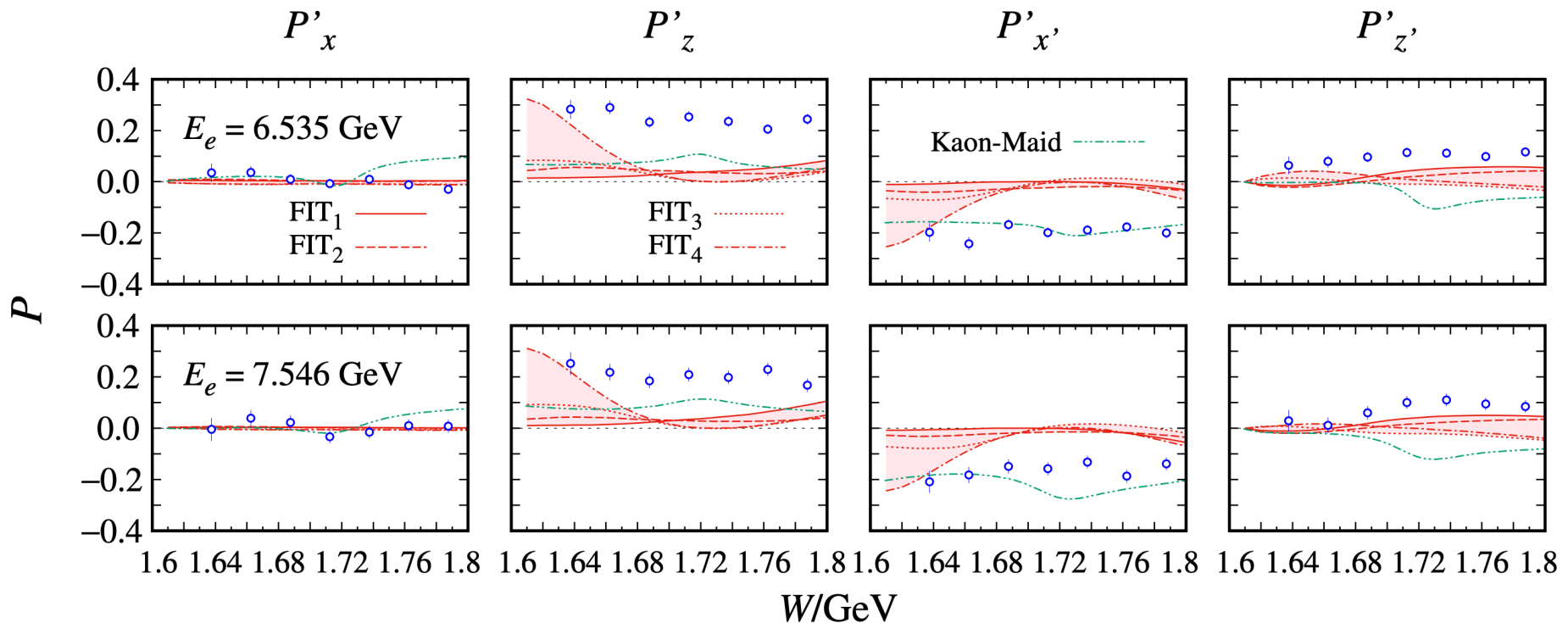




# K Λ Challenges: Polarization measurements

- During analysis, first polarization data became available by CLAS:
- Predicted, not fitted

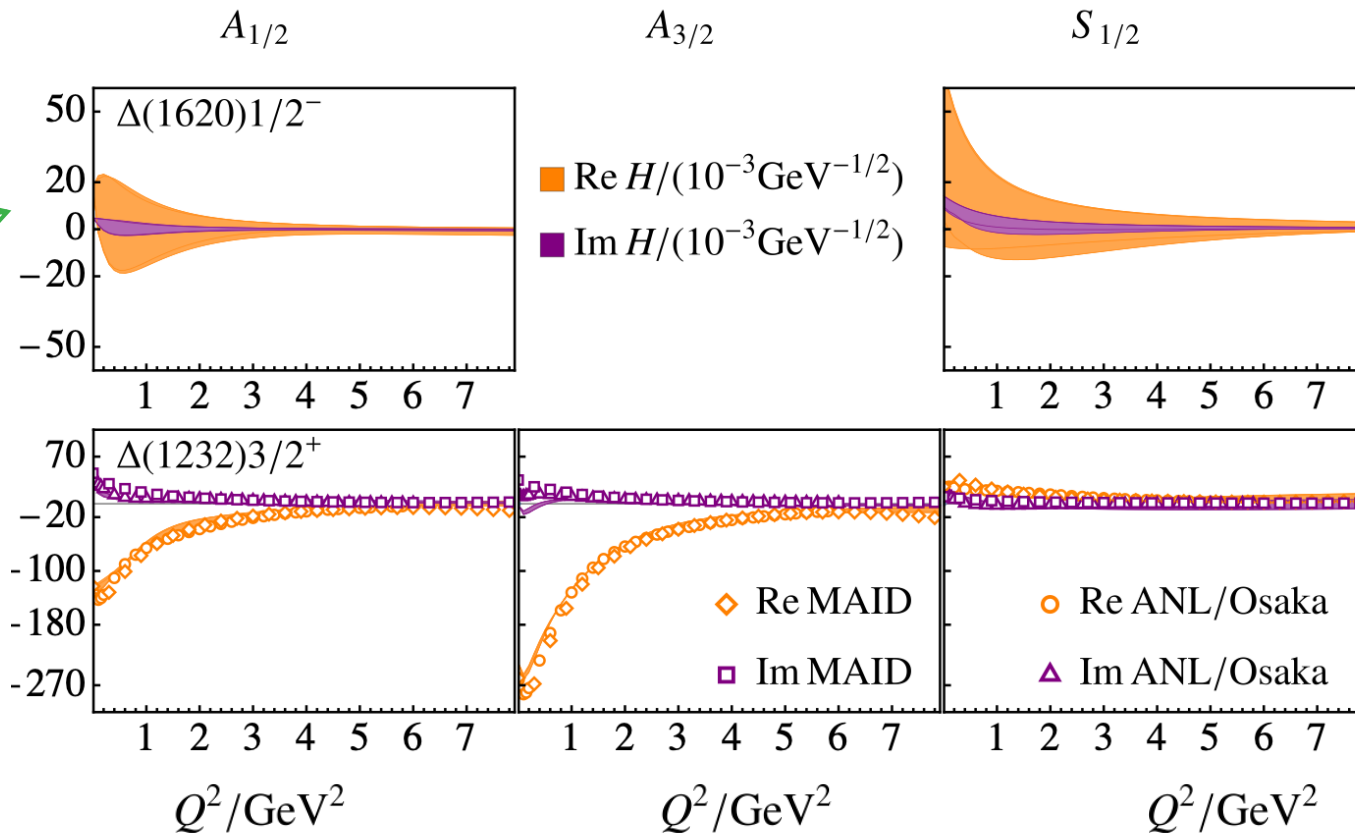
Beam-recoil polarization transfer  
[\[Carman et al. 2022\]](#)



# Helicity Couplings I

[Yu-Fei Wang et al., 2024]

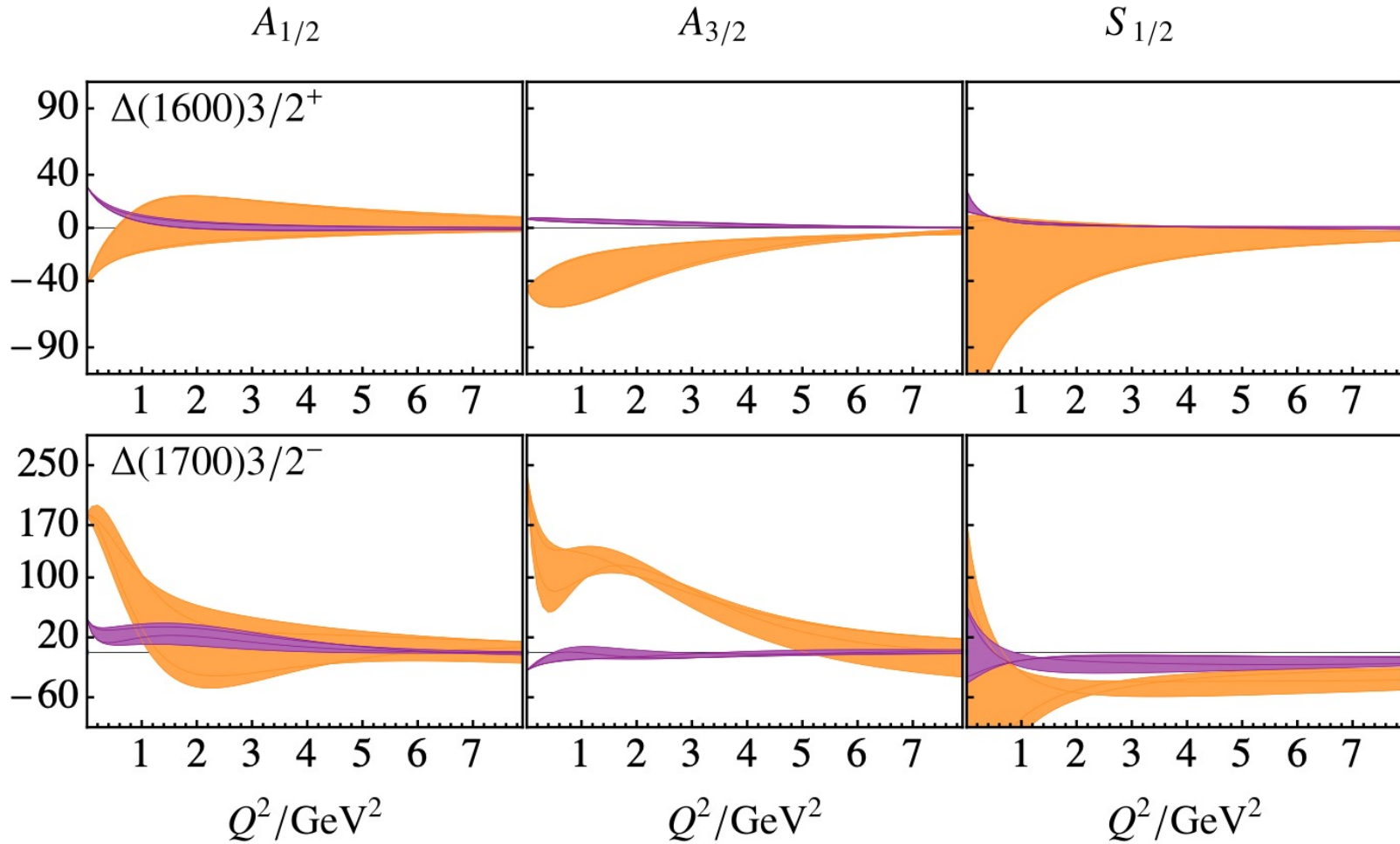
- Determined at resonance poles/ many for the first time



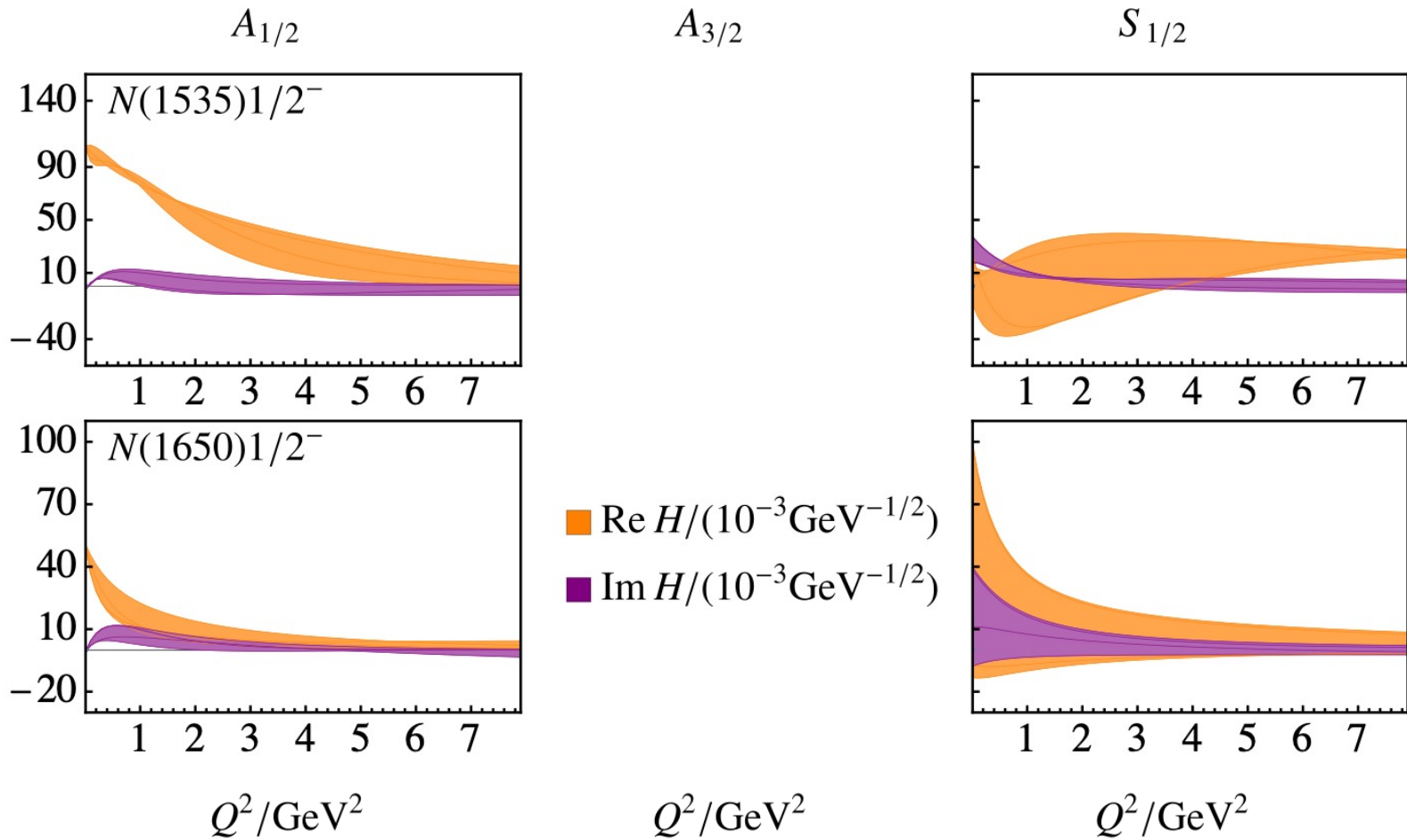
Compares qualitatively with [Mokeev et al., 2022]

# Helicity Couplings II

[Yu-Fei Wang et al., 2024]



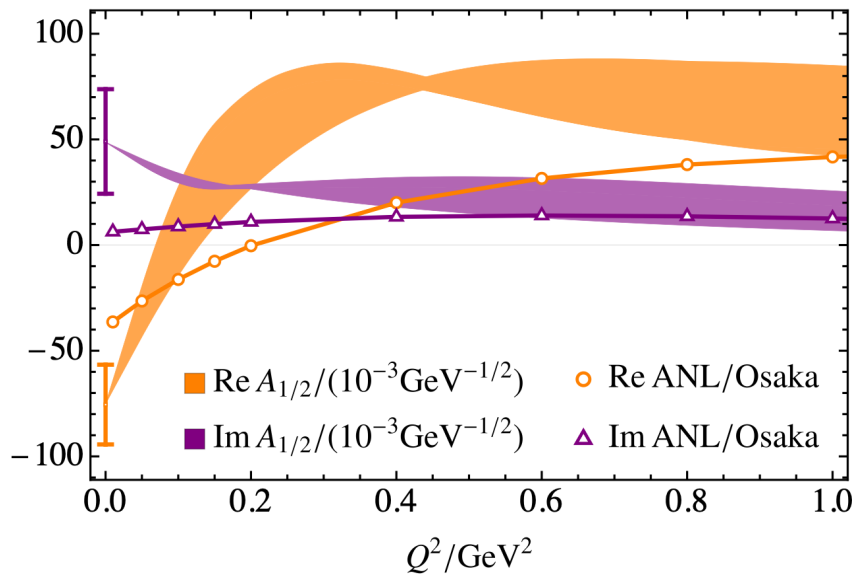
# Helicity Couplings II



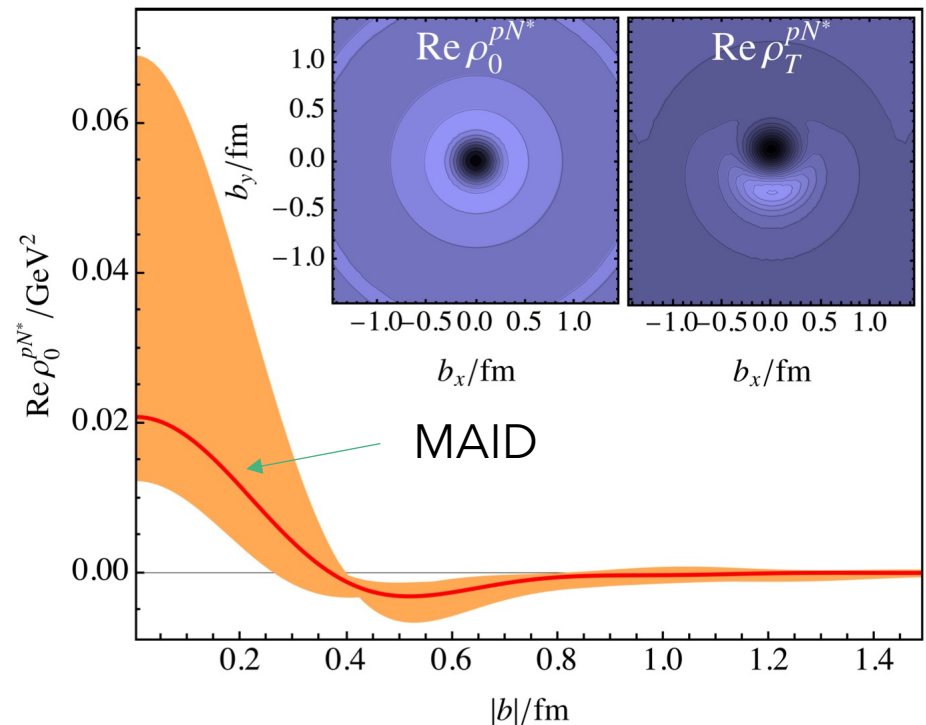
# Results for the Roper resonance

Charge density structure

[approx./ following Tiator et al., (2009)]



$$\rho_0^{NN^*}(\vec{b}) \equiv \int \frac{d^2\vec{q}_\perp}{(2\pi)^2} e^{-i\vec{q}_\perp \cdot \vec{b}} \frac{1}{2P^+} \times \langle P^+, \frac{\vec{q}_\perp}{2}, \lambda | J^+(0) | P^+, -\frac{\vec{q}_\perp}{2}, \lambda \rangle,$$



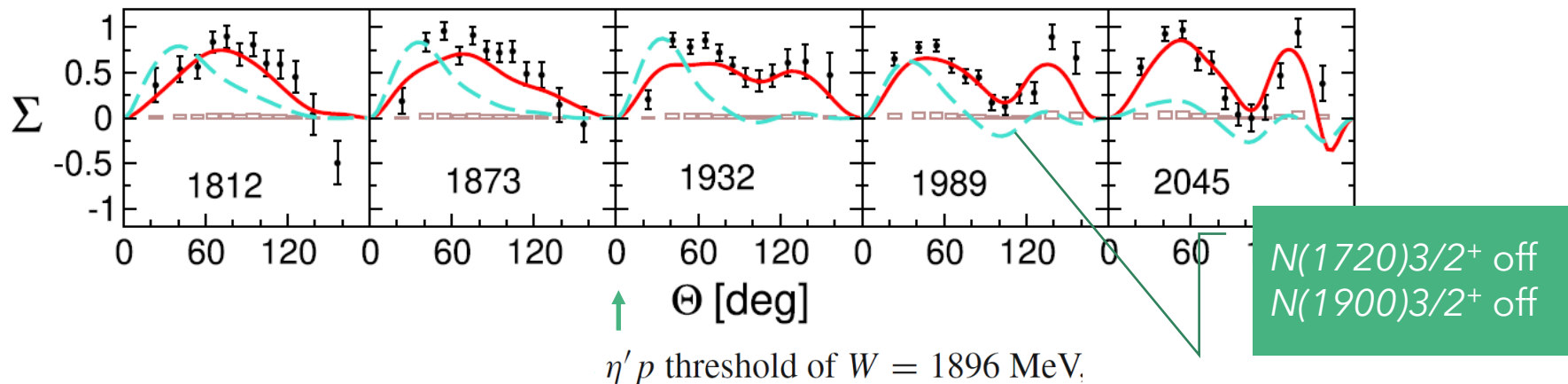
# Summary

- Juelich-Bonn-Washington/JBW model: Phenomenology of excited baryons through coupled-channels, two- and three-body dynamics.
- Renewed effort to explore additional reaction channels in the last years:
  - $\gamma p \rightarrow K\Sigma$
  - $\pi N \rightarrow \omega N$
  - $\gamma^* p \rightarrow \pi N, \eta N, K\Lambda$  (Electroproduction)
- First global electroproduction analysis of different final states
- “Extensive” exploration of parameter space with good  $\chi^2$  (better than MAID) leads to *significant* variance of some multipoles.
- Many transition form factors at the pole extracted for the first time.
- Open questions:
  - How to get solid statistical statements out of a heterogeneous data base dominated by systematic errors?
  - Blinding spectroscopy

(spare slides)

# 2022 Update in other reactions

- Beam asymmetry in  $\eta$  photoproduction (different  $W$ )



- $N(1710)1/2^+$  returns with large  $\eta N$  and  $K\Lambda$  branching ratios

